Target Representation on an Autonomous Vehicle with Low-Level Sensors

Estela Bicho

Department of Industrial Electronics
University of Minho
4800 Guimarães, Portugal
C.N.R.S.-Centre de Recherche en Neurosciences Cognitives
13402 Marseille Cédex 20, France
estela@lnf.cnrs-mrs.fr

Pierre Mallet
Gregor Schöner

C.N.R.S.-Centre de Recherche en Neurosciences Cognitives
13402 Marseille Cédex 20, France

Abstract

How can low-level autonomous robots with only very simple sensor systems be endowed with cognitive capabilities? Specifically, we consider a system that uses seven infrared sensors and five microphones to avoid obstacles and acquire sound targets. The cognitive abilities of the vehicle consist of representing the direction in which a sound source lies. This representation supports target detection, estimation of target direction, selection of one out of multiple-detected targets, storage of target direction in short-term memory, continuous updating of memory, and deletion of memorized target information after a characteristic delay. We show that the dynamic approach (attractor dynamics) employed to control the motion of the robot can be extended to the level of representation by using dynamic neural fields to interpolate sensory information. We show how the system stabilizes decisions in the presence of multivalue sensorial information and activates and deactivates memory. Smooth integration of this target representation with target acquisition, in the form of phonotaxis, and obstacle avoidance is demonstrated.

1. Introduction

Autonomous vehicles are robotic systems that are not only able to control their motion in response to the sensory information acquired by themselves but are also able to act intelligently (or flexibly) in their environment. Acting in an intelligent way requires the system to exhibit some cognitive capabilities. This means that the system must be able to behave autonomously even in response to environmental constraints not directly linked to online sensory information. Moving toward an occluded target, for instance, requires memory. That memory must be updated when sensory information is again available, or must be deleted if such information continues to be unavailable over a characteristic period of time. Making and stabilizing a decision in the presence of multivalued or ambiguous information is another form of cognitive capability, in that such decisions are not directly dictated by the incoming sensory information. We speak of representations of information when the processing of sensory information generates such cognitive capabilities.

Over the past decade or so, some controversy has existed regarding the appropriate role of representations within robotic systems. At one extreme, the use of symbolic representations has been viewed as an impediment to efficient and effective control of autonomous robots, by roboticists subscribing to a behavior-based approach (Brooks 1991; Connell 1990). On the other hand, it has long been assumed and argued that strong forms of representation are needed when robots are aimed at that perform in ways that go beyond the purely reactive (Chatila 1994). A consensus, which appears to emerge now, does not reject representations as such, but emphasizes their integration within the architecture of an autonomous robot (Arkin 1998).

The dynamic approach to autonomous robotics was developed initially as a method of planning within representations of the navigable space (Schöner and Dose 1992). The first implementations involved relatively high-level systems with ample computing power and vision as the primary source of sensory information (Schöner, Dose, and Engels 1995). For such systems, it has been shown that the approach is not limited to the realization of relatively simple control behaviors, such as obstacle avoidance and target acquisition, but may generate cognitive capacities such as subsymbolic memory

The International Journal of Robotics Research
Vol 19, No. 5, May 2000, pp. 424-447,

(Engels and Schöner 1995) or the representation of computed metric information and its association with sensory input (for ego-position estimation [Steinhage and Schöner 1997], for instance).

That there is nothing in the approach that actually requires us to work at such a relatively high level of abstraction has been demonstrated when a very low-level platform with very modest computational power and low-level sensorial information (consisting of five infrared sensors and two light-dependent resistors) was programmed to avoid obstacles and move toward light sources (Bicho and Schöner 1997a). The same dynamical systems used earlier for planning (Schöner and Dose 1992) were employed. That system was purely reactive, however, lacking cognitive capabilities.

Here we are exploring the extent to which the capacity of the dynamic approach to generate cognitive properties transfers to these lower-level platforms as well. Specifically, can continuous metric representations be derived from low-level sensory information, decisions be stabilized on such representations, and subsymbolic memory and processes operating on memorized information (e.g., suppression of outdated information) be implemented? This transfer to lower levels of sensory information is not trivial. The high-end systems deal with such cognitive functions essentially by compressing large amounts of sensory information as obtained from computer vision into reduced representations. The dynamic decision-making and memory operations could be viewed as sophisticated forms of noise removal and model-based estimation. By contrast, low-level sensors typically provide very limited amounts of sensory information. For instance, a small set of microphones provides a very *coarse-grained* sample of the ambient distribution of sound intensity. From this sample, a stable and graded representation must be derived. The nature of the problem is thus changed from information compression and noise removal toward interpolation. In both cases, integration of the representations with stable action planning and control must be achieved.

We answer these questions in the affirmative by demonstrating the cognitive properties of a simple target representation system where targets are defined as sound sources. A dynamic field representation of the spatial direction in which sound targets are detected is constructed. The robot receives sensory information from five weakly directional microphones that scan the forward 180-deg hemicircle. Input to the field is thus a two-dimensional sound panorama (direction versus intensity). A dynamic neural field representing sound target direction is endowed with the capacity to make and stabilize decisions in response to multivalued sensory information (such as when two sound sources lead to a bimodal input distribution). Strong recurrent connections in the dynamic neural field lead to subsymbolic memory that enables the robot to continue moving toward a sound source even when it is temporarily silenced. A process of adaptation is constructed that gradually reduces the stability of memorized information so that a memorized target orientation is deactivated if no confirmatory sensory information is received within a particular time span. This dynamics of target representation is coupled into a previously established dynamic architecture for target acquisition and obstacle avoidance (Bicho, Mallet, and Schöner 1998). Results obtained from the implementation prove the capacity of the system to perform target detection and localization and target selection, and to exhibit temporary knowledge (memory and forgetting). Smooth overt behavior and the ability to track and follow moving sound sources are also demonstrated.

This paper is structured as follows: In Section 2, we review some related work. Section 3 provides a review of the dynamic approach to behavior generation and simultaneously defines the target acquisition and obstacle avoidance behaviors used here. Dynamic fields for behavior representation are presented in Section 4. Next, in Section 5, the dynamic field representing sound targets is specified and its integration with the movement control architecture is explained. Some details of the implementation of this architecture on a robot platform are given in Section 6. Experimental results are described in Section 7. The paper ends with discussion and conclusions in Section 8.

2. Related Work

Moving toward sound sources is called "phonotaxis" in biology (Braitenberg 1984), and one may think of our system as a simple, although cognitive, realization of this basic behavior of organisms. Phonotaxis is exhibited by quite simple nervous systems. For example, in cricket mating, the male cricket attracts a female by generating noise. Successful mating entails detection, recognition, and localization in space of the mating sound, and movement toward the sound source (Cade and Cade 1992). This example illustrates there are two fundamental problems solved by the female cricket: The incoming sound signal must be detected and recognized as the call of a male member of the species. This detected signal must then be used to locate the source of the sound. This biological example has inspired work on low-level robots to test hypothesis and control mechanisms that account for phonotaxis in crickets (Webb 1995). An interesting robot model is reported in Lund, Webb, and Hallam (1997). They tested their robot in a number of experiments based on cricket research. They reproduce a set of behaviors including signal choice, which have often been taken as evidence for complex mechanisms that go beyond purely peripheral nervous control. In their model, however, phonotaxis is implemented through a simple control-system-like mechanism. The model does not, therefore, have any cognitive capabilities (e.g., no memory, no representation of direction other than by physically rotating the robot). The model also does not address integration of phonotaxis with other behaviors such as the avoidance of obstacles during movement toward the sound source.

A simple realization of taxis behaviors can be based on the rule of turning left if left-looking sensors detect more signal than right-looking sensors and conversely. Using nonlinear dynamical systems, this qualitative form of control can be integrated with other behaviors, in particular, with obstacle avoidance (Bicho and Schöner 1997a). Such a solution fails, however, to explicitly represent the spatial direction toward the target source. That direction is only represented implicitly by the physical orientation of the robot once the control mechanism has stabilized. The presence of other constraints such as obstacle avoidance, distorts even this implicit representation. It is therefore not possible, based on this simple algorithm, to perform additional computations on the target information, such as memorizing that information, or steering at a given angle relative to the sound source (to enable, for instance, multiple, sound emitting robots to drive in formation). Moreover, this simplest mechanism does not support explicit decision making and stabilization of decisions when sensory information is ambiguous, for instance, because sound from two different sources impinges on the sensors with comparable intensity.

There is a considerable amount of modeling work on sound localization by higher-level nervous systems, including models of spatial hearing in humans (Mills 1972; Blauert 1996; Duda 1996; Shama, Shen, and Gopalawamy 1989). Binaural processing is the mechanism through which humans (and some animals, such as, for example, the barn owl) localize sound. In humans, this entails exploiting interaural intensity differences (for the estimation of the elevation of the source) and interaural time differences (for the estimation of the horizontal orientation of the source). Some technical systems for sound localization have used arrays of microphones measuring differences between the signals received at the different microphones. An example, which was aimed at robotics as its major application, is described in Guentchev and Weng (1998). This system does not deal with multiple sources.

The approach adopted in this paper is very close to mathematical models of biological systems for target localization and selection, in which the prey localization and selection by frogs and toads (Chipalkatti and Arbib 1987; House 1988) has been described using neural fields (Amari 1977). In these species, prey catching is triggered by very low-level visual cues (Ewert 1974). These models remained somewhat limited at the time as they did not deal with continuous updating of the target representation in time, nor with the integration of such a representation into other ongoing behaviors (the goal of the models was not, of course, to create autonomous robots).

Outside the particular angle provided by analogies with biological systems, related problems are addressed in robotics in the domain of target tracking. The location, velocity, and other attributes of multiple moving objects are estimated from sensor data. Modern systems for target tracking often use multiple physically distributed sensors of different types to provide complementary and overlapping information about targets. Thus, fusion is necessary to extract the relevant information on the targets and integrate that information across different sensor systems. Functional architectures for tracking thus require the two operations of data association, establishing which sensory measurement belongs to which target, and estimation (Liggins, Kadar, and Vannicola 1997). A wide array of established methods of estimation exist. In most cases, estimates of the state of each target (e.g., position and velocity) are based on a model of the target and its motion.

Such methods have, to our knowledge, not been directly applied to the problem of estimating the direction in which a sound source lies. This may be due, in part, to the limited practical importance of this problem for the target-tracking community. A more fundamental problem may be, however, that a good model of sound propagation is difficult to establish without taking recourse to a substantial amount of measurements to establish the geometry and reflective properties of the environment.

3. Behavior Generation through Attractor Dynamics

In this section, we describe the method used to implement target acquisition and obstacle avoidance and provide, on that occasion, a brief review of the basic principles of the dynamic approach to behavior generation (see Schöner, Dose, and Engels 1995; Bicho 1999, for a review):

(1) *Behavioral variables* are used to describe, quantify, and internally represent the state of the system with respect to elementary behaviors. For target acquisition and obstacle avoidance of an autonomous vehicle moving in the plane, the *heading direction*, ϕ ($0 \leq \phi \leq 2\pi$), with respect to an arbitrary but fixed world axis, is an appropriate behavioral variable (Schöner and Dose 1992). As is illustrated in Figure 1, the direction, ψ_{tar}, in which a target lies as seen from the current position of the robot, specifies a desired value for heading direction. Directions, ψ_{obs}, in which obstacles lie specify values of heading direction that must be avoided.

(2) Behavior is generated by continuously providing values to the behavioral variables, which control the robot's effectors. The time course of these values is obtained from solutions of a dynamical system. The attractor solutions (asymptotically stable states) dominate these solutions by design. In the present system, the *behavioral dynamics* of heading direction, $\phi(t)$, is a differential equation

$$\frac{d\phi}{dt} = f(\phi) = f_{\text{obs}}(\phi) + f_{\text{tar}}(\phi) \tag{1}$$

built from a number of additive contributions that express task constraints. Each constraint is cast either as a repulsive (Fig. 2) or as an attractive force-let (Fig. 3), which are both characterized by three parameters: (a) which value of the behavioral variable is specified (e.g., ψ_{obs} or ψ_{tar});

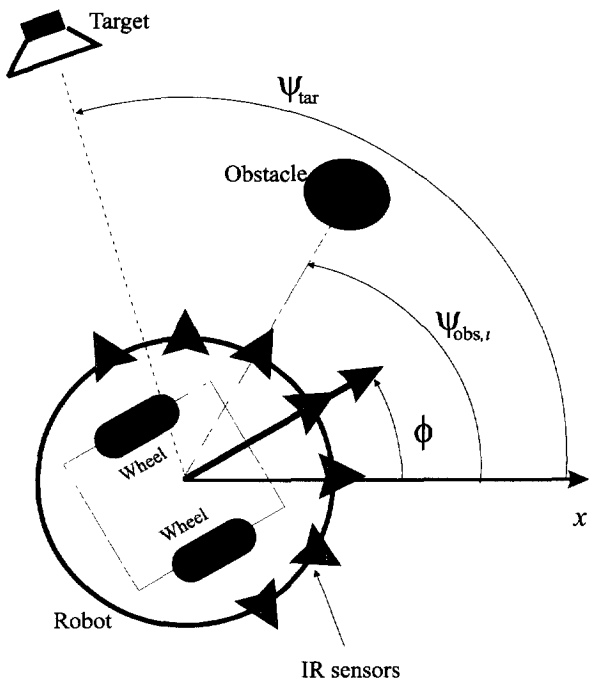

Fig. 1. The heading direction, ϕ, of the robot is defined relative to an arbitrary, but fixed, external reference frame centered in the robot. The environment specifies desired (ψ_{tar} for targets) or undesired ($\psi_{obs,i}$ for obstacles) values of this variable.

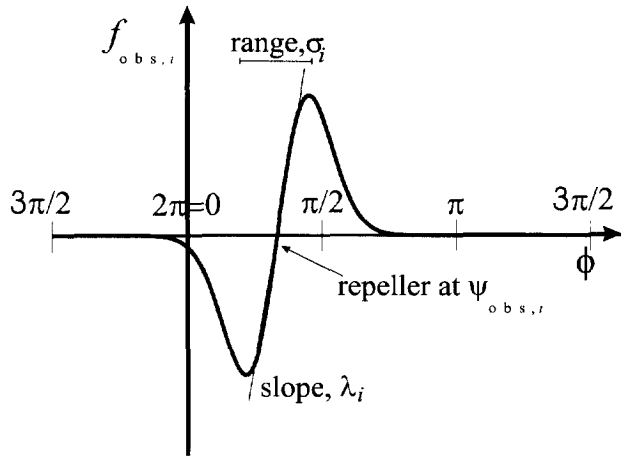

Fig. 2. A contribution to the dynamics of heading direction expressing the task constraint "avoid moving toward obstacles" is a force-let with a zero-crossing at the direction, $\psi_{obs,i}$ at which an obstacle has been detected. Every distance sensor ($i = 1, 2, \ldots, 7$) contributes such a force-let centered on the direction in which the sensor points. The positive slope of the force at the zero-crossing makes that direction a repellor. By decreasing this slope with increasing measured distance, only nearby surfaces repell strongly. The range of the force-let is limited based on sensor range and on the constraint of passing without contact.

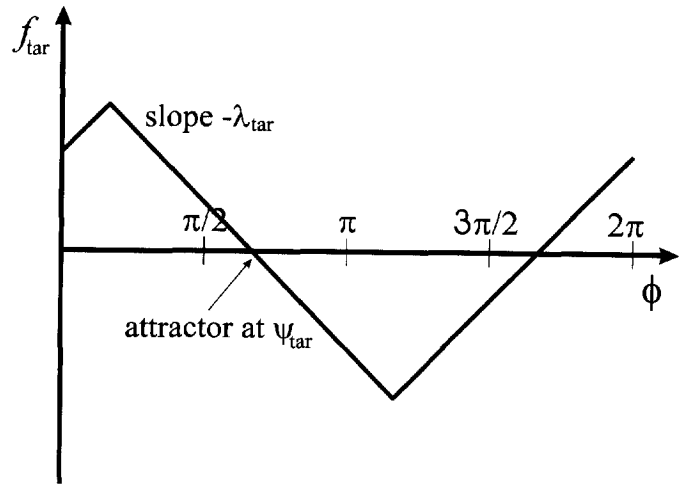

Fig. 3. A contribution to the dynamics of heading direction expressing the task constraint "move toward target" is a force with a zero-crossing at the specified direction toward the target, ψ_{tar}. The negative slope at the zero-crossing makes this an attractor of the dynamics. The target contribution is piecewise linear and extends over the entire range of heading direction. This leads to a repellor in the direction $\pi + \psi_{tar}$ opposite to ψ_{tar}.

(b) how strongly the repulsion or attraction effect is, and (c) over which range of values of the behavioral variable this force-let acts. Thus, in isolation, each force-let erects an attractor (asymptotically stable state) or a repellor (unstable state) of the dynamics of the behavioral variable. An attractive force-let serves to attract the system to a desired value of the behavioral variable (here the direction in which a target lies). A repulsive force-let is used to avoid the values of the behavioral variable that violate a task constraint (here the directions in which obstacles lie). Note that a repulsive force-let erects two semiattractors at the left and right boundaries of the repulsive zone (corresponding to passing on the left or right of the obstacle).

This method of constructing a behavioral dynamics can be used on systems with low-level sensors by defining a force-let for each sensor (Bicho and Schöner 1997a). The three parameters defining each force-let are obtained from sensory input. For example, the robot used in this project has seven infrared sensors mounted on a ring that is centered on the robot's rotation axis. These infrared sensors are used to measure the distance to surfaces at the height of the robot, which are thus obstacles. Each sensor ($i = 1, 2, \ldots, 7$) contributes a repulsive force-let

$$f_{obs,i} = \lambda_i(\phi - \psi_{obs,i}) \exp\left[-\frac{(\phi - \psi_{obs,i})^2}{2\sigma_i^2}\right] \quad (2)$$

illustrated in Figure 2. Here $\psi_{obs,i}$ is the direction in the world in which sensor i is pointing. As the heading direction, ϕ, is defined relative to the same reference frame, the relevant

difference, $\phi - \psi_{\text{obs},i} = -\theta_i$ is actually a constant, the inverse of the angle, θ_i, at which the IR sensor i is mounted relative to the forward direction of the robot.

This illustrates that the calibration of the robot's heading direction in the world is irrelevant. The strength of repulsion, λ_i, of each contribution is a decreasing function of the sensed distance, d_i, estimated from the IR sensor reading:

$$\lambda_i = \beta_1 \exp[-d_i/\beta_2]. \tag{3}$$

The parameter β_1 determines the maximal strength of this contribution, while β_2 fixes the distance over which the repulsive contribution decays. The larger the sensed distance to any obstruction detected by IR sensor i, the weaker the repulsion from the direction in which this sensor is pointing in space. The angular range over which the contribution acts is determined by σ_i, which also depends on the sensed distance, d_i:

$$\sigma_i = \arctan\left[\tan(\Delta\theta/2) + \frac{R_{\text{robot}}}{R_{\text{robot}} + d_i}\right]. \tag{4}$$

The first term reflects the angular range, $\Delta\theta$, over which the IR sensor detects reflected infrared radiation, while the second term expresses the angular safety margin required for the robot of size, R_{robot}, to pass next to an obstacle that could occupy maximally the entire sensor range. The larger the distance to the obstacle, the smaller the angle subtended by a copy of the robot when positioned next to the obstacle and viewed from the robot's actual position, and hence, the smaller the angular safety margin.

Orientation toward a target that has been detected at direction ψ_{tar} (for example, by the target representation system we introduce in Section 5) is brought about by erecting an attractor at this direction with strength λ_{tar}. Because target acquisition is desired from any starting orientation of the robot, the range over which this contribution exhibits its attractive effect is the entire full circle, i.e., from 0 to 2π rad. As a consequence, there is a repellor at the back, in the direction opposite to that toward the target (see Fig. 3). A simplest mathematical form can be piecewise linear

$$f_{\text{tar}} = \begin{cases} -\lambda_{\text{tar}}(\phi - \psi_{\text{tar}}) \\ \text{for } \psi_{\text{tar}} - \pi/2 < \phi \le \psi_{\text{tar}} + \pi/2 \\ \lambda_{\text{tar}}(\phi - \psi_{\text{tar}} - \pi) \\ \text{for } \psi_{\text{tar}} + \pi/2 < \phi \le \psi_{\text{tar}} + 3\pi/2 \end{cases}, \tag{5}$$

where ϕ value is mapped into the listed cases through a *modulus* 2π operation.

The target contribution and the contributions arising from the detected obstacles all act at the same time. The heading direction dynamics is thus simply the sum over these:

$$\frac{d\phi}{dt} = \sum_{i=1}^{7} f_{\text{obs},i} + f_{\text{tar}}. \tag{6}$$

More sophisticated control over activation and deactivation of such contributions can be obtained using activation networks (see Steinhage and Schöner 1997; Steinhage 1998; Large, Christensen, and Bajcsy 1999) but is unnecessary here. Since some of the force-lets have limited range, this superposition is a nonlinear dynamical system, which may have multiple attractors and repellors (typically few). By design, the system is operated so that the heading direction is in a resulting attractor of this dynamics most of the time. Thus, the behavior is really generated by an attractor solution and not by a transient solution of the dynamical system. This way we avoid the very difficult problem of designing a nonlinear dynamical system all transient solutions of which fulfill multiple constraints. By contrast, designing a dynamical system, the attractors of which fulfill particular constraints, is possible by making use of the qualitative theory of dynamical systems (Perko 1991). Local bifurcation theory helps to make design decisions around points, at which the system must switch from one type of solution to another (Schöner, Dose, and Engels 1995). The values of model parameters can be chosen in part based on such analyses.

Up to this point, we have only addressed the control of the vehicle's heading direction. For the robot to move, it must have some path velocity, of course. As it moves, sensory information changes and thus attractors (and repellors) shift. The same happens if obstacles or targets move in the world. Since the system must be in or near an attractor at all times, for the design principle to work, the rate of such shifts must be limited to permit the system to track the attractor, staying close to a stable state. One way this can be accomplished is by controlling the path velocity, v, of the vehicle. For resting environment and constant heading, the maximal rate of change of obstacle or target bearing, $\dot{\psi}_{\max}$, occurs when the corresponding objects are seen at a right angle to the current heading, in which case $\dot{\psi}_{\max} = v/d$, where d is the distance to the object and v is the path velocity. This approximate description can be turned around to compute the desired velocity as a function of distance with $\dot{\psi}_{\max}$ as a design parameter, that can be tuned to obtain good tracking. Because distance estimates are based on different mechanisms for obstacles and targets, we compute the desired velocity separately for each of the two constraints (i = tar or obs):

$$V_i = d_i \dot{\psi}_{\max}. \tag{7}$$

For the target constraint, the distance to the target is estimated from sound intensity. This measure is completely uncalibrated, of course, as it depends on the unknown intensity of the sound source. The determination of the proportionality constant, $\dot{\psi}_{\max}$, is thus an empirical matter. The desired velocities are imposed through a very simple linear dynamics (Bicho and Schöner 1997a)

$$dv/dt = -c_{\text{obs}}(v - V_{\text{obs}}) - c_{\text{tar}}(v - V_{\text{tar}}). \tag{8}$$

The strengths, c_{obs} and c_{tar}, are adjusted such that in the presence of strong obstacle contributions the obstacle term dominates while in the absence of such contributions the reverse holds. A systematic way to construct a function that indicates if obstacle contributions are present is to integrate the obstacle force-lets, from which something like a potential function of the obstacle avoidance dynamics results:

$$U(\phi) = \sum_{i=1}^{7} \left(\lambda_i \sigma_i^2 \exp[-(\phi - \psi_{obs,i})^2 / 2\sigma_i^2] - \lambda_i \sigma_i^2 / \sqrt{e} \right). \tag{9}$$

Positive values of this potential function indicate that the heading direction is in a repulsion zone of sufficient strength, λ_i, so $c_{obs} > 0$ and $c_{tar} = 0$ are required. Conversely, negative values of the potential indicate that the heading direction is outside the repulsion range or repulsion is weak, so now $c_{obs} = 0$ and $c_{tar} > 0$ are required. The transformation of levels of the potential to the strengths of the two contributions to velocity control makes use of a sigmoidal threshold function, $\alpha(\phi) = \arctan[cU(\phi)]/\pi$ ranging from $-1/2$ to $1/2$:

$$c_{obs} = c_{v,obs}(1/2 + \alpha(\phi)) \tag{10}$$

$$c_{tar} = c_{v,tar}(1/2 - \alpha(\phi)). \tag{11}$$

At sufficiently sharp sigmoids (c sufficiently large), this leads to the required transition behavior. The parameters, $c_{v,tar}$ and $c_{v,obs}$, determine the relaxation rate of the velocity dynamics in the two limit cases when either the obstacle or the target constraints dominate. The following hierarchy of relaxation rates ensures that the system relaxes to the attractors and that obstacle avoidance has precedence over the target contribution:

$$\lambda_{tar} \ll c_{v,tar}, \quad \lambda_{obs} \ll c_{v,obs}, \quad \lambda_{tar} \ll \lambda_{obs}. \tag{12}$$

4. Dynamic Fields for Representation

More abstract forms of behavior or processes cannot be realized with attractor dynamics of the type described above. Examples in the present context are (1) Target detection, in which a target is indicated only if sensory information is sufficiently strong and convergent while the absence of a target is signaled for weak or disperse sensory information; (2) Interpolation, that is, the capacity to make continuous estimates of the target location when sensory information is provided by a discrete array of sensors; (3) Computations on distributed representations of sensory information in which multiple instances of a sensed quality exist or sensory information is ambiguous; (4) Memory, that is, the representation of information about a target location, during transient occlusions from the sensors, so that overt behavior can be generated that continues to move the robot toward the target; (5) Forgetting, that is, the gradual deactivation of a memorized target location if no confirmatory sensory information is received within a particular time span.

Such processes, which we continue to refer to as behaviors, although they do not necessarily involve overt movement, entail representations of information. Dynamical systems of the type presented above have a unique state at all times (each variable has exactly one value) and change state continuously in time (to attain a new value, each variable must pass through all intermediate values). Such dynamical systems are thus incapable of representing graded amounts of information about a behavioral variable. For instance, the absence of any knowledge about a particular variable cannot be expressed, nor can the presence of ambiguous, multivalued information in a manner that does not yet reflect a decision.

The concept of a dynamic field of activation was proposed to overcome this limitation (see Engels and Schöner 1995; Schöner, Dose, and Engels 1995, for a review). In a first step, behavioral variables are now conceived of as behavioral dimensions, spanning a space of possible values of these variables. Over that space of behavioral dimensions, a field of activation is defined. At each location of the field, the level of activation represents the extent to which the particular value of the behavioral variable is presently specified, which is coded into the location along the behavioral dimension. Well-defined states of the behavioral variable are thus represented by peaks of activation, centered over the appropriate location in the field, that is, at the specified values on the behavioral dimension.

For phonotaxis, we want to represent the direction, ψ, in which a sound source lies, as viewed from the robot but referenced to an external frame. This variable can take on values in the interval $[0, 2\pi]$ rad. An activation variable, $u(\psi)$, is thus defined for each possible value of target direction, ψ. The function $u(\psi)$ is now the dynamical state variable and "codes" if a target in direction, ψ, is detected. Positive values of activation, $u(\psi) > 0$, indicate that a target near ψ is detected; negative values of activation, $u(\psi) <= 0$, indicate that no target was detected near ψ. The larger the activation, the more certainty about detection of a target. A single target is thus represented by a single localized peak of activation in the field (Fig. 4, top). The absence of information on a possible target is expressed through a homogeneous state of the field ($u(\psi) <= 0$ everywhere) (Fig. 4, bottom).

The second step is to lift the ideas about attractor dynamics and bifurcations to the level of a dynamics of the entire field. Localized peaks of activation are made attractor solutions by a particular pattern of interactions in the field. Sensory information provides input to the field. We develop these ideas step by step.

Assume that the readings of the sound sensors at time t are given as an input sound distribution, $S(\psi, t)$. (In practice, the sensor readings at a small number of field locations,

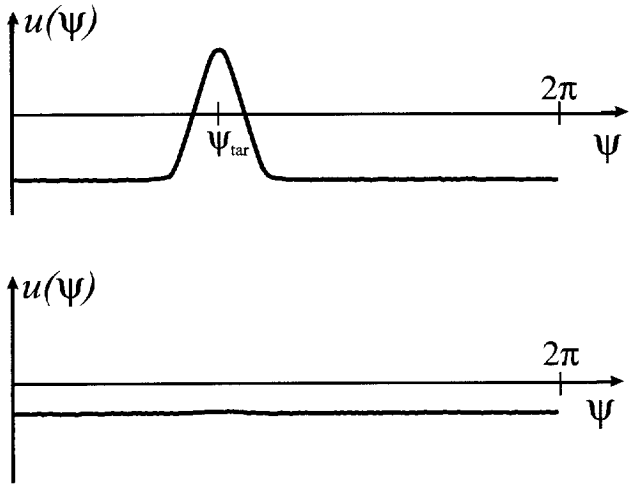

Fig. 4. A field of activation is defined over the *behavioral dimension*, ψ, of the direction in which a target is detected. (a) A localized peak of activation represents a single target in the direction, ψ_{tar}, corresponding to the location of the peak. (b) A flat, subzero level of activation represents the absence of target information.

ψ, are convolved with a Gaussian filter so that they activate continuous regions of the field, see Section 5.) The simplest dynamics is one in which all sites of the field evolve independently of each other toward a level of activation, $u(\psi, t)$, that reflects the amount of input at each site:

$$\tau \frac{du(\psi, t)}{dt} = -u(\psi, t) + S(\psi, t). \tag{13}$$

This linear dynamics makes the field relax to the current input pattern, $u(\psi) = S(\psi)$, with a low-pass characteristic. This dynamics is thus not yet useful by itself, as it merely reproduces the shape of the input pattern. What we need are mechanisms that make that activation in the field become positive only when a critical amount of input is given (detection), that activate only one site if multiple sites receive similar input (selection), and that are capable of retaining activation after input is removed (memory). In the last case, it becomes particularly clear that such mechanisms involve *interaction*, that is, the evolution of activation at one site of the field depends on the level of activation at other sites of the field.

An interaction mechanism that does the job has three characteristics: (1) Neighboring field sites provide each other with positive input ("local excitation"). (2) Field sites at larger distances provide each other with negative input ("global inhibition"). (3) Only field sites with positive activation contribute to interaction ("sigmoid threshold"). Localized peaks of activation are thus lifted up by local excitation. This makes it possible to sustain localized peaks of activation even once input has been removed. That is the basis of memory. Moreover, when input creates a localized peak, there is a critical amount of activation when the local excitation first sets in and beyond which the peak can be self-sustained. This is the basis of detection. If there are multiple sites that receive input, global inhibition sets in. As soon as one field site has gained even only a minute advantage in activation, it wins the competition and suppresses other sites more than it is suppressed itself. This is due to the sigmoid, which weakens the influence of sites with lower levels of activation.

A convenient mathematical format of this interaction mechanism is

$$\tau \frac{du(\psi, t)}{dt} = -u(\psi, t) + S(\psi, t) + \int_0^{2\pi} w(\psi - \psi')\Theta(u(\psi', t))d\psi' + h. \tag{14}$$

Interaction collects input from all field sites, ψ'. The sigmoid threshold function

$$\Theta(u) = \begin{cases} 0 & \text{for } u < 0 \\ u & \text{for } 0 < u < 1 \\ 1 & \text{for } u > 1 \end{cases} \tag{15}$$

makes sure that only sites of the field with positive activation contribute to interaction. The interaction kernel

$$w(\Delta\psi) = \begin{cases} k_p & \text{for } -l_{\text{coop}} < 2\Delta\psi < l_{\text{coop}} \\ -k_n & \text{else} \end{cases} \tag{16}$$

only depends on the distance, $\Delta\psi = \psi - \psi'$, between field sites. It is positive ($k_p > 0$) if the two sites are closer to each other than the cooperativity length, l_{coop}, and is negative ($k_n > 0$) for larger distances. The kernel is shown in Figure 5. Finally, the negative constant, $h < 0$, determines the resting level of the field without input: $u = h$ everywhere. This controls how much input field sites need before they first contribute to interaction.

This equation can be viewed as a neural network with continuously many neurons. It was first proposed in the 1970s to model activity patterns in the cortical surface, in which a very large number of interacting neurons creates a network that is almost homogeneous along the cortical surface and can thus be approximated as a continuous field of neural activation (Wilson and Cowan 1973; Amari 1977). The particular form of the equation we are employing has been analyzed mathematically by Amari (1977) and by Kishimoto and Amari (1979). Their work provides valuable information about the different regimes of stability and the role of the different parameters for the existence and stability of localized activity patterns.

4.1. Detection

The resting level, $h < 0$, makes sure that interaction kicks in only when sufficient input is applied. For an input, $S(\psi)$,

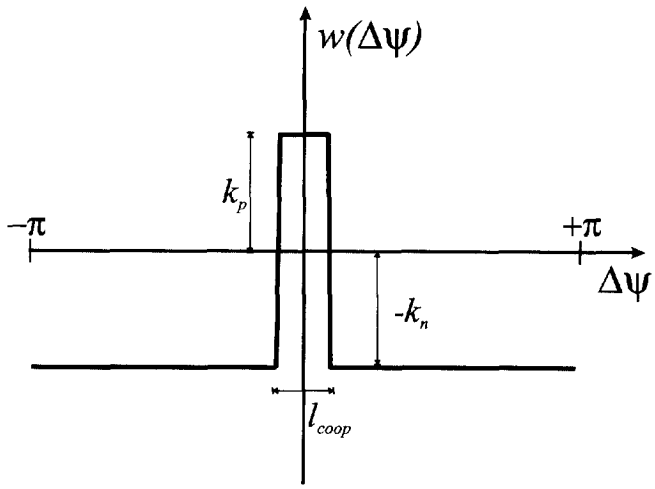

Fig. 5. The interaction kernel is positive ("excitatory") for sites that are closer to each other than the cooperativity length, l_{coop}, and is negative ("inhibitory") for larger distances between the sites.

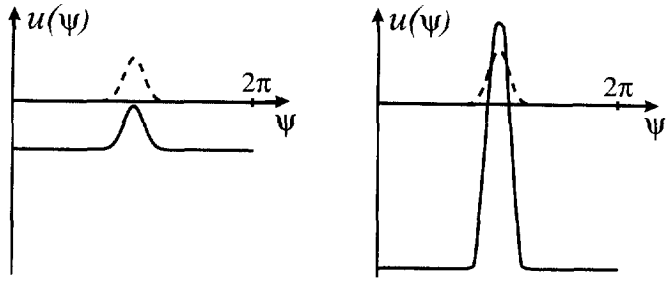

Fig. 6. A single localized input, $S(\psi)$, is applied to the field (dashed line). Left: When the amplitude of that input is below a critical level, the stable state of the field is the homogeneous resting level with the input profile superposed: $u(\psi) = h + S(\psi) < 0$ (solid line). Right: Beyond a critical input amplitude, activation in the field becomes positive and interaction sets in. The stable state that emerges (solid line)is a localized peak of positive activation, which is largely self-sustained but positioned over the location of maximal input. The transition between these two states is hysteretic and represents the detection mechanism.

localized around one location, for instance, this means that while that input has a small amplitude, the homogeneous state of the field is deformed by the input but remains negative everywhere: $u(\psi) = h + S(\psi)$, as illustrated in Figure 6 on the left. The field codes absence of information (no target detected). When the amplitude of input is sufficiently strong, interaction becomes important. The stable state of the field is now a localized peak of positive activation, the size of which not only reflects input strength but is also determined in large part by local self-excitation. The transition between the subthreshold peak and the self-sustained peak as a function of input strength involves a dynamical instability and is the mechanism used here for detection. Detection means that input needs to be of sufficient size over a sufficient period of time to generate a self-sustained peak. The location of the self-sustained peak is determined entirely by input; however, the peak is positioned over the location of maximal input.

4.2. Memory

Once a localized, positive peak of activation has been generated, the local self-excitation within the peak is so strong that a peaked pattern of activation remains stable even after input is removed (Fig. 7). This is the dynamic field mechanism for memory. This form of memory is subsymbolic. Within the category of memory, defined by the behavioral dimension, ψ, an instance of memory is identified simply by its location. There is no need to label peaks. When input information is reapplied, the position of the stable peak is readjusted so as to be centered exactly on the location of maximal input. Thus, memory is updated automatically without need for an explicit input-to-memory matching process.

Over the longer term, memorized information may become obsolete. Angular information may become incorrect because

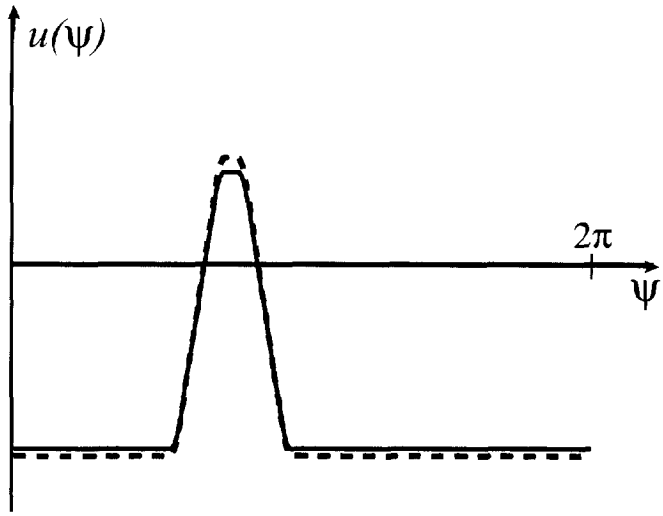

Fig. 7. A localized positive peak of activation (dashed line) is stable in the presence of input. It remains stable if input is removed (solid line). The peak is sustained by local self-excitation. Its lateral diffusion is limited by global inhibition. This is the memory mechanism in the dynamic field. The position of the peak within the field is marginally stable, however, so that the contents of memory may slowly degrade with time.

the robot moved. Targets may actually have been removed. Even the memory mechanism itself is subject to degradation as the peak position within the field is only marginally stable in the absence of input. A mechanism for forgetting must suppress positive localized peaks of activation if no confirmatory sensory input arrives within an appropriate time interval.

The resting level, $h < 0$, provides such a mechanism. When the resting level is made sufficiently negative, activation in the field is generally so low that the local self-excitation is no longer sufficient to sustain a positive peak of activation. In fact, mathematically, the field dynamics without input goes through an instability when the resting level is varied (Amari 1977). At levels of h below but close to zero, the field dynamics is bistable: the homogeneous "off" state of the field coexists with the state in which a localized positive peak of activation is positioned somewhere within the field. This is the regime in which memory is operational: If input has induced a positive peak of activation and is then removed, the system maintains a localized peak of activation. If no input has been present, the homogeneous off state persists. When the resting level is lowered below a critical value ($h < -W_m = -\max_\psi\{\int_0^\psi w(\Delta\psi)d\Delta\psi\}$), the localized positive peak solution becomes unstable and the field dynamics is monostable, with only the homogeneous off state remaining. Thus, a localized memory peak can be deleted by lowering the resting level below this critical level. The two regimes of the field dynamics are illustrated in Figure 8.

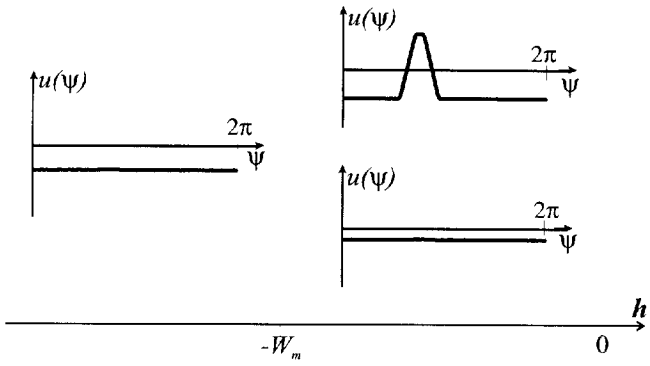

Fig. 8. The different stable states of the field dynamics without input are illustrated as a function of the resting level, h. Below a critical level of h ($-W_m$), only the homogeneous "off" state of the field is stable. All sites have the same negative level of activation. Above the critical level (but still below zero), two types of stable states coexist. The homogeneous state persists, but a positive localized peak of activation is likewise stable (irrespective of where it is positioned). This bistable regime serves the memory function, while the monostable regime induces forgetting or resetting of memory. Memory peaks are set by applying sufficiently strong input (see detection mechanism).

4.3. Decision Making

When more complex shapes of input distributions are considered, additional properties of this strongly interactive field come into play. The top of Figure 9 shows that bimodal input patterns may lead to a single localized peak of activation that is positioned over the mean of the two locations of maximal input. This is, in fact, a weighted mean as different amplitudes of the two input peaks lead to bias of the resulting position of the localized peak of activation toward the site receiving stronger input (left). This fusion or integration of input information results from the local excitatory interaction. Roughly, when the two peaks of the input distribution are within the cooperative length, l_{coop} of the dynamic field, then fusion takes place as shown.

If, by contrast, the two peaks of the input distribution are separated by more than the cooperative length, then a decision is made as to which peak to activate. The field is bistable. A positive localized peak may be positioned over either of the two sites. The other site remains more activated than the background but is suppressed below zero (bottom of Fig. 9). Which of the two sites of maximal input "wins" depends on two factors: (a) The initial state of the field may bias the competition toward maintaining positive activation where there has previously been positive activation. This leads to hysteresis, in which a decision once made is stabilized in the face of multivalued or ambiguous information. (b) If the two input peaks have different amplitude, then the site receiving stronger input is more likely to be activated.

5. The Dynamics of Target Representation

To build a dynamic field representation of the sound sources, we use the direction, ψ, in which the sound source lies as viewed from the current position of the vehicle. The angle is taken relative to a fixed but arbitrary reference orientation, so that it would not change if the robot were to turn on the spot. In implementation, this requires integrating heading direction in time to maintain this reference frame. While the absolute calibration of this reference frame is irrelevant, its drift contributes to degradation of memorized information but not of currently sensed information. A much more limiting factor of this form of target representation is that memorized angular information becomes obsolete as the robot moves over distances comparable to the distance to the target. The main advantage of this representation is, however, that distance information is not needed for detection, estimation, decision making, and short-term memory of targets.

A dynamic field, as defined in the previous section, represents information about the orientation of a potential sound target. Sensory input to the field is provided by the time-varying signals, M_i, from five microphones ($i = 1, 2, \ldots, 5$), each pointing into a different sector on the forward field of view of the vehicle (angles $\zeta_i = (-90, -45, 0, 45, 90$ deg)

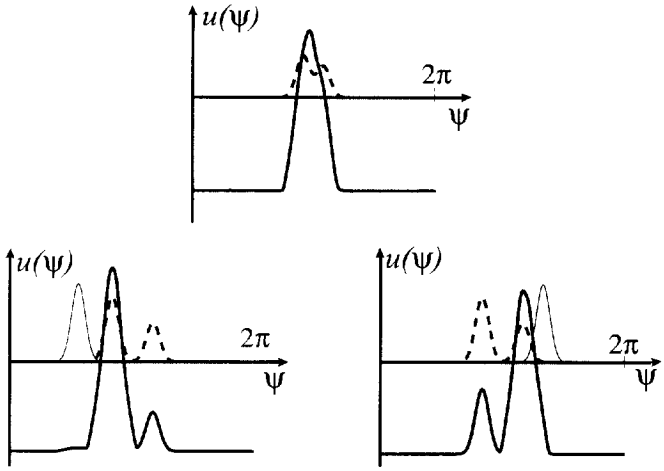

Fig. 9. A monomodal input, $S(\psi)$, is applied to the field (dashed line). Top: when the distance between the two peaks of the input distribution is within the cooperative distance, the stable state of the field is a localized peak of activation (solid bold line) positioned over the weighted mean of the input distribution. The field thus fuses input information. Bottom: when the distance between the two peaks of the input distribution is beyond the cooperative distance, competition takes place. The field is bistable, in the sense that it can evolve a peak of activation centered at either one of the two sites receiving input (solid bold line). On the left, the site receiving stronger input "wins." On the right, the initial state of the field (solid thin line) has a peak of activation at a distance to the smaller peak, within the cooperative distance, the competition is thus biased toward the selection of the smaller input peak.

from the main axis of the vehicle, see Fig. 10). These signals reflect the sound pressure measured by each microphone. They increase from zero with increasing sound pressure. Their angular characteristic is described approximately by a cone of about a 60-deg opening, so that neighboring microphones have overlapping sensitivity cones. Thus, these sensors specify target orientation in the sense that a single sound source induces a graded pattern of detected sound pressure, with a maximum at the sensor pointing in the direction closest to the one in which the sound source lies (except for reflections, see Section 7). Interpolation is based on spreading the contribution of each microphone over a range in the field by convolving with a Gaussian kernel of width, $\sigma = 0.4$ rad (±23 deg):

$$S(\psi, t) = \left(\sum_{i=1}^{5} M_i \exp\left[-\frac{(\psi - \psi_i)^2}{2\sigma^2} \right] - M_o \right) H\left(\sum_{i=1}^{5} M_i \right). \tag{17}$$

Here, $H(\cdot)$ is the Heaviside step function. Multiplying with this step function applied to the sum of all microphone signals turns input entirely off when no sensor receives input (background sound below sensor threshold).

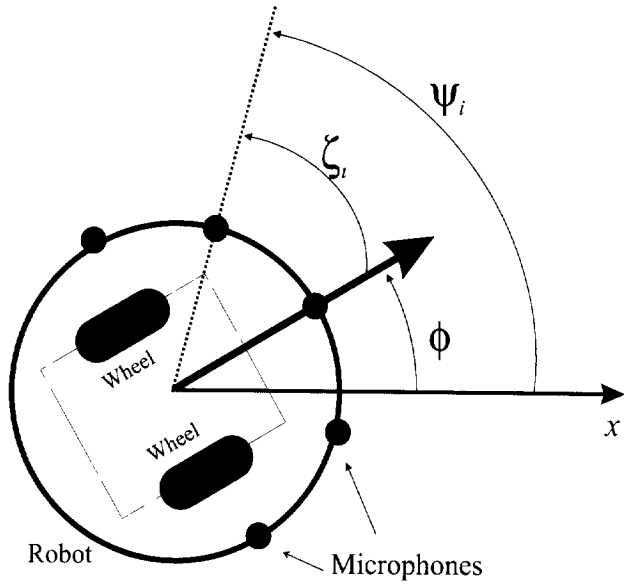

Fig. 10. Sensory information about sound targets is acquired by five microphones, each pointing into a direction ζ_i (= −90, −45, 0, 45, 90 deg), with respect to the heading direction, ϕ, of the robot. The direction in the world at which microphone i is pointing is $\psi_i = \phi + \zeta_i$.

The parameter h is set so that the field operates in the memory mode. Thus, once sufficient input (detection) has induced a single localized peak of positive activation (decision), that peak persists when input is removed (e.g., because the sound source is momentarily silent or its volume is reduced due to occlusion). The memorized target orientation is maintained for a time interval that permits the robot to continue moving in the target direction. This memory peak must be deleted if no renewed sensory input arrives within a particular period of time, as memorized angular information becomes obsolete as the robot moves. This forgetting behavior is modeled by making the resting level, h, a dynamical variable with the following dynamics:

$$\frac{dh}{dt} = -r_{h,\min} c_h (h - h_{\min}) - r_{h,\max} (1 - c_h)(h - h_{\max}). \tag{18}$$

Here, $h_{\max} = -0.125 W_m$ and $h_{\min} = -1.1 W_m$ are the two limit values of the resting level within the bistable and the monostable regime, respectively (see previous section and Fig. 8 for significance of W_m). This dynamics lowers the resting level (destabilizing memory) at the rate $r_{h,\min}$ while a memorized peak exists ($c_h = 1$). It restores the maximal resting level (to enable memory) at the rate $r_{h,\max}$ otherwise. The destabilization (forgetting) process is slower than the restoring process, so that after forgetting, the field is immediately able to again detect and memorize a new target. The presence of a memorized peak is represented by

$$c_h = [H(N_u) - H(N_s)]H(N_u), \tag{19}$$

where

$$N_u = \int_0^{2\pi} H(u(\psi))d\psi \tag{20}$$

is the total positive activation in the field and

$$N_s = \int_0^{2\pi} S(\psi)d\psi \tag{21}$$

is the total input activation (positive by construction). $H(\cdot)$ is the heaviside step function. The function c_h is equal to 1 if there is positive activation in the field ($N_u > 0$), but no input ($N_s = 0$). It is zero if there is no peak in the field or if there is a peak but also input.

Now we address how the direction, ψ_{tar}, in which a target lies, can be computed from the activation on the dynamic field. Because the time scale, τ, of the field is chosen faster than that of the heading direction and velocity dynamics ($1/\beta_1$), the field has typically relaxed to a stable pattern on the time scale on which the movement plans of the robot evolve. Directly reading out the location in the field of maximal activation is not a very good solution, as the maximum of the stable state may jump and thus destroy the carefully constructed stability properties of the system. Moreover, such a procedure does not deal consistently with the absence of target information. A better and elegant solution has been proposed by Kopecz and Schöner (1995) and used in an earlier implementation of dynamic fields on vehicles (Bicho and Schöner 1997b). Because the field has by construction only a single peak of positive activation, the peak location could be computed as a mean, if the distribution of activation is interpreted as a probability density

$$\psi_{\text{tar}} = \int_0^{2\pi} \psi H(u(\psi))d\psi / N_u, \tag{22}$$

where division by the total positive activation, N_u, is needed to normalize the distribution. The normalization poses a problem when no positive activation exists in the field. This problem can be solved once it is realized that what we actually need in the dynamics of heading direction is not necessarily ψ_{tar} itself, but $-\lambda_{\text{tar}}(\phi - \psi_{\text{tar}})$, an attractive force-let centered at that angle. The strength of attraction must be zero if no target is represented. Thus, λ_{tar} should be replaced by $\lambda'_{\text{tar}} N_u$ with a new constant, $\lambda'_{\text{tar}} > 0$. This leads to $-\lambda'_{\text{tar}}(N_u\phi - N_u\psi_{\text{tar}})$, in which the normalization factor cancels and division by zero never occurs. Thus, we redefine the target contribution as

$$f_{\text{tar}} = \begin{cases} -\lambda'_{\text{tar}}(N_u\phi - \int_0^{2\pi}(H(u(\psi))\psi)d\psi) \\ \text{for } \psi_{\text{tar}} - \pi/2 < \phi \le \psi_{\text{tar}} + \pi/2 \\ \lambda'_{\text{tar}}(N_u(\phi - \pi) - \int_0^{2\pi}(H(u(\psi))\psi)d\psi) \\ \text{for } \psi_{\text{tar}} + \pi/2 < \phi \le \psi_{\text{tar}} + 3\pi/2 \end{cases}. \tag{23}$$

6. Implementation on the Robot

The dynamic architecture was implemented and tested on the mobile platform depicted in Figure 11. The vehicle was designed and built by one of us (P. M.) at the CNRC in Marseille. It consists of a cylindrical platform with two lateral motorized wheels and a passive rear caster wheel. Sensory information is acquired from seven infrared (IR) detectors (distance sensing for obstacle avoidance) mounted on a first ring, and five directional microphones (sound intensity sensing for phonotaxis) mounted on a second ring. These two rings are centered on the axis connecting the two active wheels.

The IR sensors are active (emitter and receiver) and are sensitive to distances up to about 60 cm. They are sensitive to reflected IR light from within an angular range of about 30 deg. They are arranged along the ring such that their sensitivity cones just touch. The distance estimate derived from the IR signal is roughly calibrated in the laboratory but depends on the unknown reflectivity of surfaces in the robot's environment.

The microphones are of the cardiod type. They are most sensitive to sound arriving from the direction at which they are pointing in space. Sensitivity decreases for sound impinging from other directions. Sensitivity loss (in the mounted configuration) is about 6 dB for sound sources sideways from the microphones and 20 dB for sound sources at the rear. Microphones are spaced 45 deg apart on the upper ring around the robot.

The robot has a single board computer system based on a 486DX4 processor operating at 100 MHz, equipped with 4 Mb of DRAM and 4 Mb of FLASH memory. All control and computation is done on-board. The operating system is DOS 6.22. The algorithm was implemented in Microsoft Quick basic V4.5 (the only compiler that could be installed on the 4 Mb of FLASH memory).

The two lateral wheels are each driven by a DC brushless servomotor, each separately controlled by electronic circuitry that guarantees accurate control of rotation speed without the use of external shaft encoders. The relationship between input voltage and rotation speed is approximately linear, so that generating desired robot speeds and turning rates is easy.

In the implementation, the neural field dynamics as well as the dynamics of heading direction and of path velocity are integrated numerically using the Euler method.

The field is sampled spatially with a sampling distance of 8 deg. It is important that the discretized form of the

Fig. 11. The robotic platform.

interaction kernel, $w(\Delta\psi)$, is, like the exact kernel, symmetrical around zero. Deviations from symmetry generate a tendency for localized memory peaks to drift in one direction. Sensory information is acquired once per computation cycle. The cycle time is measured and is approximately 110 ms. As the time step must be smaller than the fastest relaxation time on the system, this imposes minimal time scales on the entire dynamical architecture. Thus, the computational cycle time is the limiting factor for determining the relaxation times of the dynamics in real time units and thus for the overall speed at which the robot's behavior evolves.

The rate of change of heading direction obtained from the dynamics of heading direction (eq. 1) directly specifies the angular velocity of the robot for rotation around its center. This can be translated into the difference between left and right wheel rotation speed. The path velocity, v, specifies the average rotation speed of both wheels. Together, the rotation speeds of both wheels can be computed and are sent as set points to the velocity servos of the two motors.

7. Experimental Results

In this section, we first present results that document the properties of the dynamical field for target representation. These were obtained when the field evolved in response to actual physical stimulation by sound sources but the robot did not move. Next we show how the robot behaves in a number of experimental scenarios that challenge particular aspects of the architecture. In all cases, all behavioral modules are integrated and work together.

7.1. Cognitive Properties of the Dynamic Field Representing Targets

A set of experiments with fixed robot used a sound source that emitted a pulse-modulated wave with a fundamental frequency of 440 Hz. Pulse modulation makes sure that this sound had high-frequency harmonics that fell into the most sensitive range of the microphones. In experiments involving multiple targets, a sound generator emitting a 2.5 KHz harmonic wave was used as a second sound source. The loud speakers were placed 100 cm from the robot. The robot was pointing in the 180-deg direction relative to the external reference frame in which we provide information about the real direction to the sound source.

7.1.1. Detection

Figure 12 shows how the field evolves when the intensity of the test sound was increased gradually. Initially, the entire field is "off" ($u(\psi) = -h < 0$ everywhere). While sensory input is weak, positive activation cannot arise and the field continues to code for absence of a sound source. At time $t \approx 55$ sec, the strength of sensory input becomes sufficiently strong to trigger generation of a peak of positive activation centered over the location that receives maximal input. From this point on, a target is detected and the peak of activation maintains its shape almost invariant due to the strong cooperativity within the field. This result shows that the dynamic field behaves nonlinearly in response to ambient sound of different intensities.

7.1.2. Interpolation

In the presence of a single sufficiently strong sound source, input is monomodal, although broad, and a single, localized positive peak of activation is stable in the dynamic field (Fig. 13). The peak is positioned over the maximum of the broad input distribution and thus unaffected by input that is further removed from the peak than the kernel width. The estimated sound orientation, ψ_{tar}, is 115 deg, very close to the actual target orientation, which was 112.5 deg. Repeating this experiment for a number of different orientations of the sound source, we evaluated the quality of the interpolation of sound input by the dynamic field. Figure 14 summarizes the result. The estimated values of target direction are very close to the real values across a wide range from 110 to 250 deg. The two extremal configurations have a small bias (still less than 10 deg), which is caused by the unsymmetric sampling of

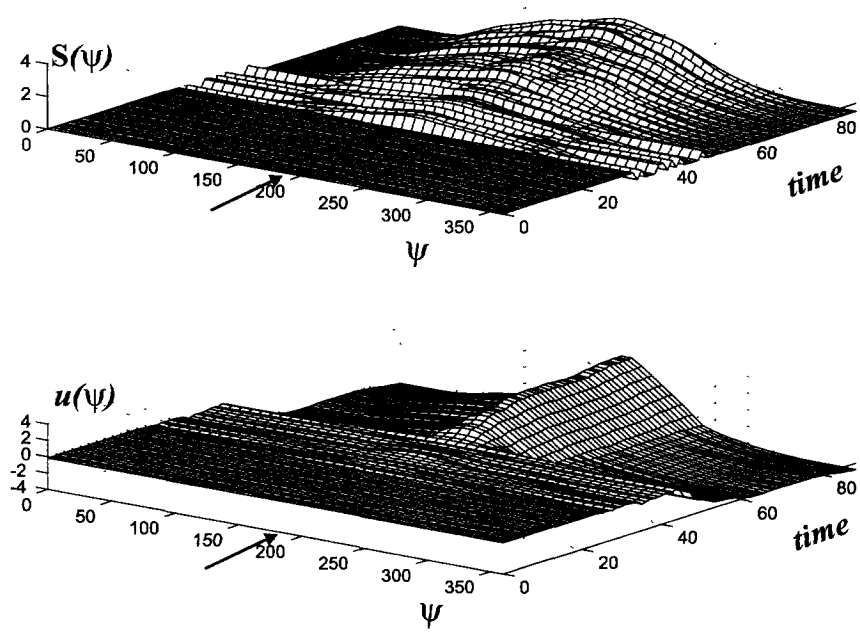

Fig. 12. Here, the target detection behavior of the field is shown. Direction is in degrees (deg) and time in seconds (sec). The sound source was placed in the forward direction of the robot (indicated by the arrow), and sound intensity was increased from 0 to 2.5. Robot position and orientation (180 deg with respect to the world axis) in space was kept fix. Top: the input to the field, $S(\psi)$, is monomodal and its strength increases in time. Bottom: while the input is weak, the field is in the state in which it is all off and thus no target is detected. At time $t \approx 55$ sec, the input strength is sufficiently strong to trigger the detection of the sound source. From this point on, the stable state of the field is a localized peak of positive activation centered over the location of maximal input.

these values due to the limited angular range of our microphone array.

7.1.3. Tracking

Figure 15 shows how a moving sound target is tracked. The loud speaker was moved more or less continuously from an initial orientation at 90 deg all the way to 270 deg. As a consequence, sensory input has a moving peak. The dynamic field responds to such moving input by evolving a peak of activation that tracks and follows the moving input peak. The maximum of the field activation moves continuously with the angular location of the target. The estimated target location thus varies monotonically from approximately 102 deg to 261 deg.

7.1.4. Target Selection

To test the capacity of the field to select one of multiple targets, two loud speakers were placed as illustrated in Figure 16. The loud speaker on the left of the robot emitted the pulse-modulated test sound while the loud speaker on the right emitted the harmonic wave of 2.5 KHz. Both signals were played at similar intensity. Input is bimodal under these conditions. The interaction enables the field to make a decision, in this case, of selecting the site receiving stronger input. The field evolves a single localized peak of positive activation centered near the input peak located near 270 deg. This input information pertaining to the alternate site is discarded and does not bias the estimation of the target position.

7.1.5. Memory and Forgetting

Memory and forgetting is demonstrated in Figure 17. A loud speaker was placed in front of the robot (it could have been any other orientation). After a brief moment of silence, the sound source was turned on, emitting the pulse-modulated test sound. As expected, the field evolved a stable peak of positive activation centered over the input peak (the estimated target orientation is 183 deg). About 10 sec later, the sound source was turned off. Although sensory input is thus removed, the localized peak persists, if somewhat weakened, for a certain time interval. During this time interval, the adaptive dynamics of the resting level, h, drives the resting level down, and thus progressively destabilizes the memorized information. Since no renewed sensory information is provided again, the memorized peak eventually dies out. The target orientation is "forgotten." At this point, the adaptive dynamics of h changes and its value is quickly restored to the value at which the

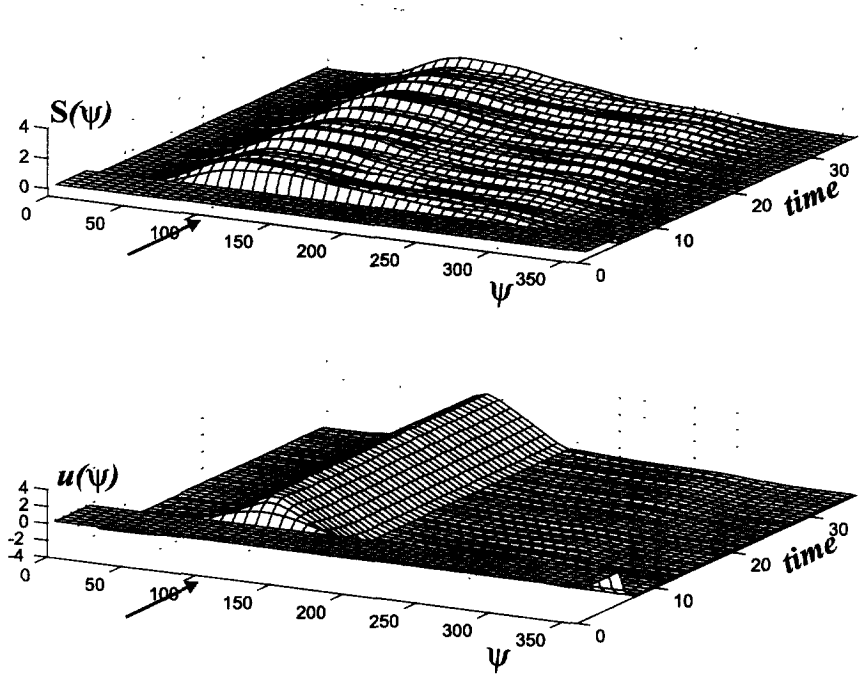

Fig. 13. A sound source was placed at an angular position of 112.5 deg (the location indicated by the arrow) with respect to the world axis. Robot orientation was 180 deg; the five microphones where thus pointing in the directions 90, 135, 180, 225, and 270 deg. Top: sensory information leads to a broad monomodal input distribution. Bottom: the field activation relaxes to a stable localized peak centered over the maximum of the input. The estimated sound orientation is 115 deg.

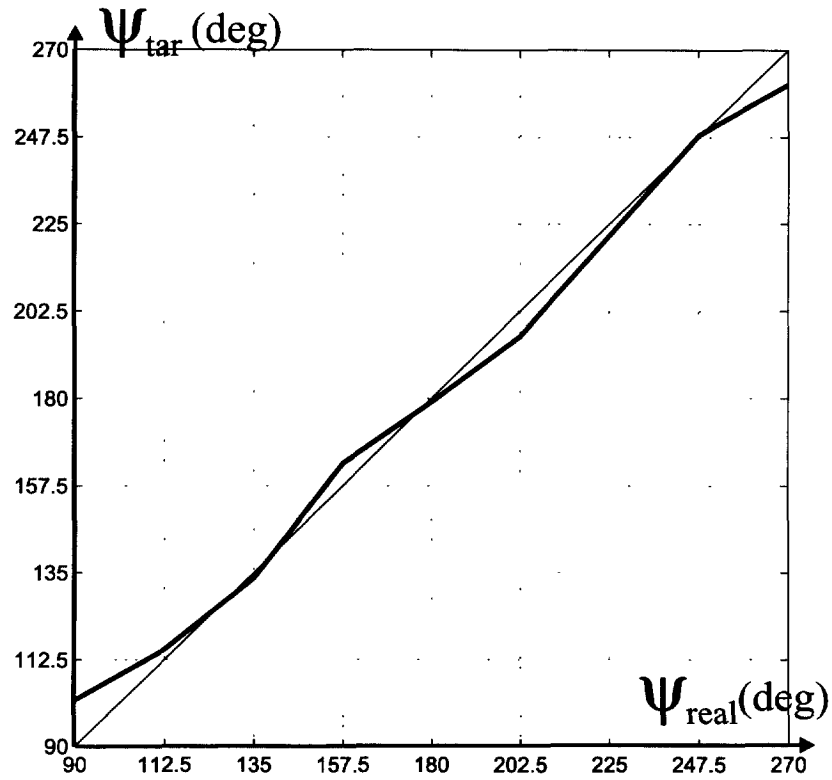

Fig. 14. The experiment illustrated in Figure 13 was repeated for a number of different directions of the sound source. These directions can be read on the abscissas. On ordinates, one can read the corresponding estimated target directions.

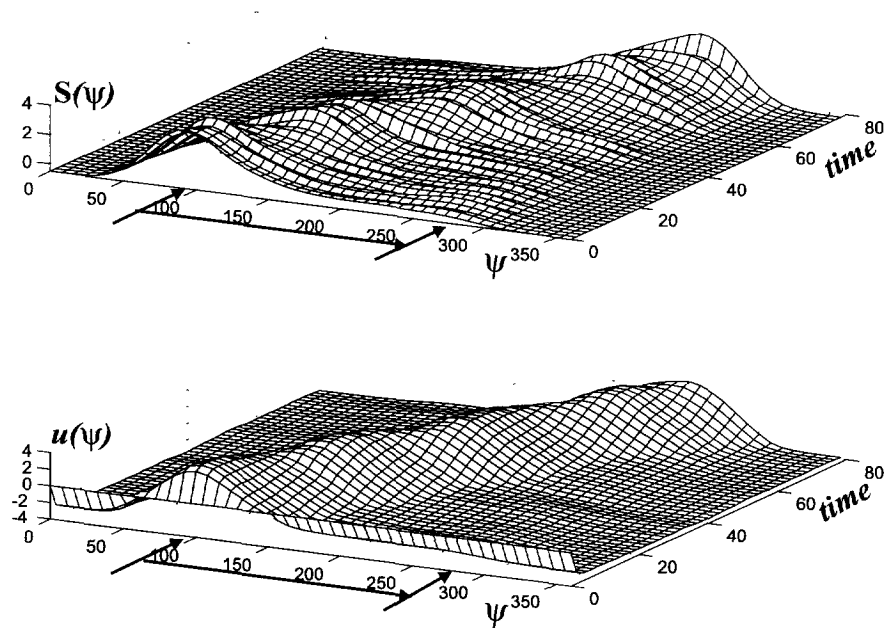

Fig. 15. The robot was positioned with an orientation of 180 deg with respect to the external axis. The sound source was moved continuously from an initial direction of 90 deg (indicated by the left arrow) all the way to 270 deg (indicated by the right arrow). Top: sensory information is monomodal and its maximal location varies continuously. Bottom: the field evolves a peak of positive activation that tracks and follows the moving input peak.

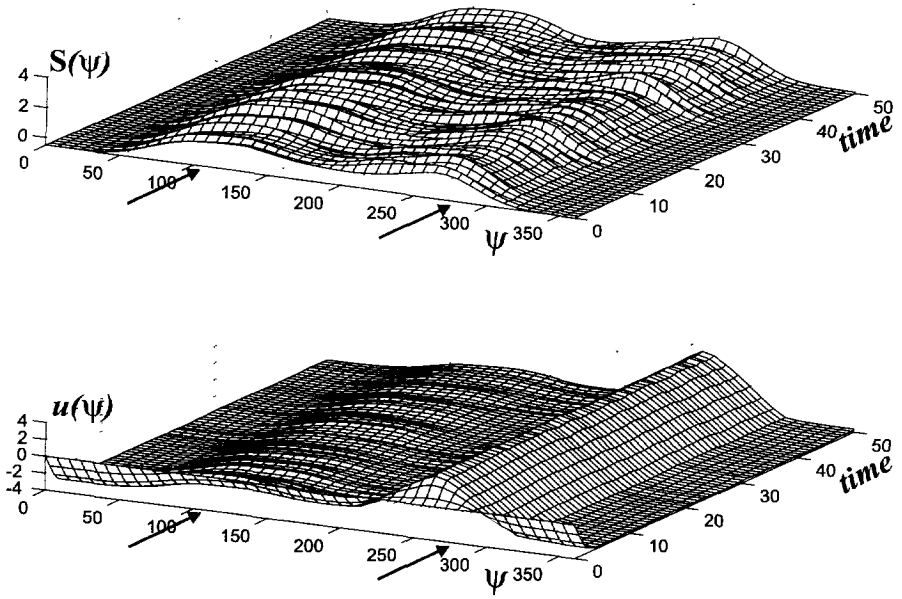

Fig. 16. The robot was placed with a heading direction of 180 deg with respect to the external axis. Two sound sources, the pulse modulated wave and the harmonic wave, were placed at angular positions 112.5 deg and 270 deg (as indicated by the arrows), respectively. Top: under such experimental setup, the sensory input to the field is bimodal. Bottom: competition takes place and as a result the field makes a decision. The field evolves a single peak of positive activation centered near the input peak located at 270 deg. Thus, the left target is selected.

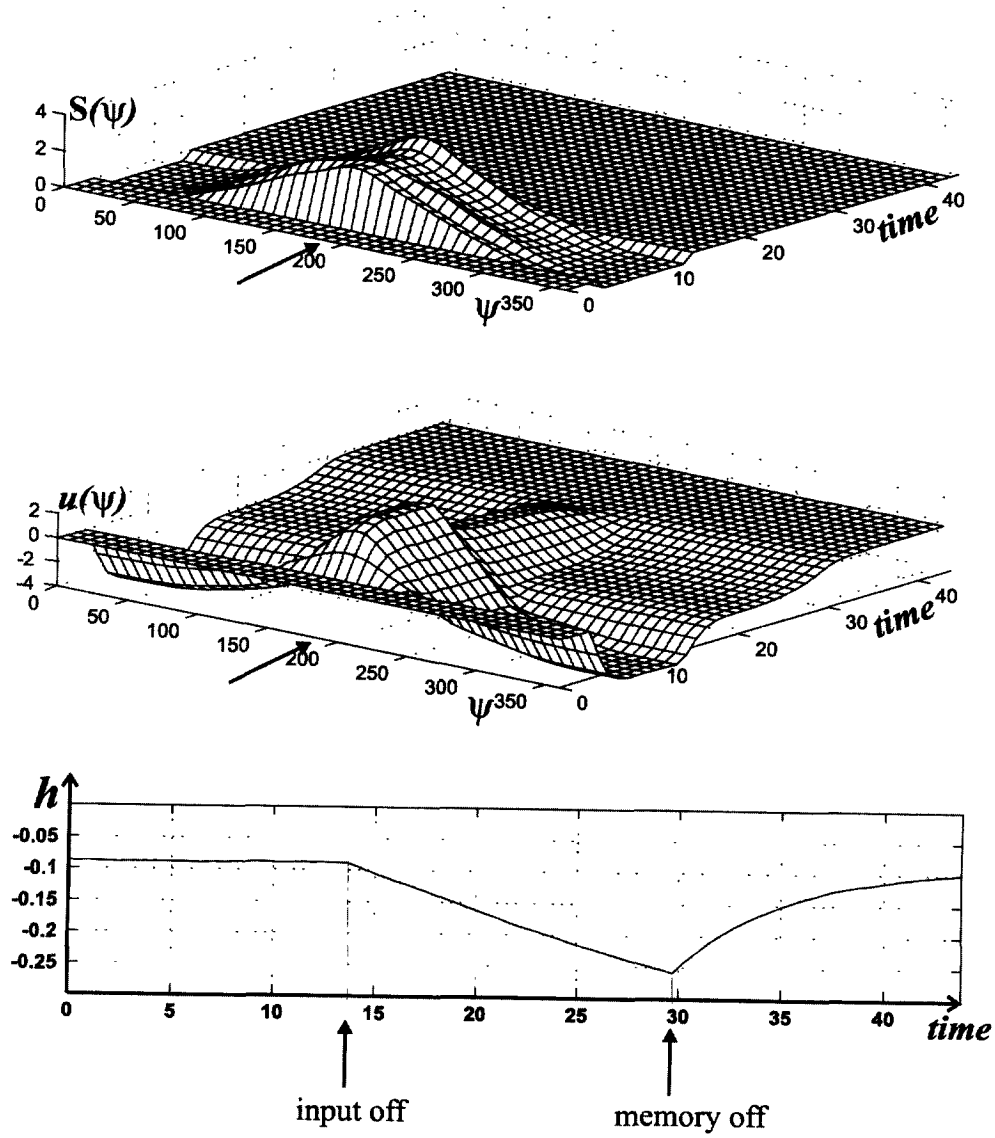

Fig. 17. A loud speaker was placed in front of the robot heading direction (indicated by the arrow). Top: 3 seconds later, the sound source was turned on. The sensory input to the field is monomodal. About 10 seconds later, the sound source was turned off. The sensory input becomes zero everywhere. Center: while the sound source is on, the state of the field is a localized peak of positive activation centered over the location of maximal input. This peak solution persists (even though somewhat reduced in amplitude) even when the input to the field is turned off ($t \approx 13$ sec). The field is thus in the memory regime. At time $t \approx 29$ seconds, this peak solution becomes unstable due to the adaptation of the resting level, h. Target orientation is thus "forgotten." From this point on, the field remains in the state in which it is off (negative activation everywhere). Bottom: the resting level is in its maximum value until the input is turned off, which occurs at time $t \approx 13$ seconds. After this instant and while there exists positive activation in the field, the adaptive dynamics of h reduces its value. At time $t \approx 29$ seconds, the resting level reaches the value for which the peak solution in the field corresponding to the memorized information becomes unstable. Thus, the memorized peak is turned off. At this point, the adaptive dynamics of h changes again and its value is restored to the value at which the field dynamics operates in the memory regime again.

target representation dynamics operates in the memory mode again. The field is once again sensitive to new (or the same) sound targets, which can be detected, selected, and memorized. Memory together with the adaptation of the resting level thus endows the robot with temporary knowledge about the target location.

7.2. Phonotaxis and Obstacle Avoidance on Moving Robot

In all the experiments reported here, the sound source consisted of a loudspeaker emitting CD music. The particular piece we used (Vivaldi, Printemps, Allegro) not only provides sound at the higher frequencies to which our microphones are sensitive but also has moments of silence that give occasion to test the memory capability of the target representation. To demonstrate target selection, the music was played through two loudspeakers.

7.2.1. Scenario with a Single Sound Source

Figure 18 illustrates the robot's behavior in the simplest scenario testing obstacle avoidance in conflict with the phonotaxis behavior. The target was a single loudspeaker placed behind a barrier (from the point of view of the initial position of the robot). The robot moves along a smooth, curved path around the obstacle to reach the target. It is the temporary knowledge about target direction retained in the dynamic field that enables the robot to continue moving in the correct direction during the periods of silence of the music. Two runs in the same scenario are shown. On one occasion, the robot goes around the obstacle to the left, on the other to the right. The heading direction dynamics is bistable in this case, and small fluctuations in sensory information can bring about either of the two paths. Once heading direction is in one of the two attractors, however, this decision is stabilized. In both cases, the target is reached and the robot comes almost to rest near the loudspeaker.

7.2.2. Scenario with Two Sound Sources

Figure 19 shows target selection based on different input strength. Two speakers were fed with the same input signal. The robot is placed initially at position A (see first frame) with the sound sources switched off. The robot moves straight ahead driven by pure obstacle avoidance. At point B (third frame), the sound sources are turned on. When the sound sources are at different distances from the robot, the closer one is always selected. Figure 20 shows that when both sound sources are at quite exactly the same distance, the decision may depend on random fluctuations of the input stream.

Target selection based on prior activation patterns (hysteresis) is demonstrated in Figure 21. Two sound sources are both behind obstacles (as seen from the initial position of the vehicle). In one run, the robot is initially closer to the sound source on the left. The field therefore establishes a peak at the leftmost target direction. The obstacle configuration forces the robot to pass through a position in which the robot receives symmetric input from the two sound sources. The preexisting peak on the left makes the robot retain the leftmost target. Analogously, when the robot starts out closer to the right target, that target is represented in the dynamic field. The robot persists in the selection while it passes through the same position as in the first run with approximately symmetric input.

7.2.3. Global Behavior

In Figure 22, we illustrate behavior in a more complex environment. Initially, the robot is positioned in the corridor of our lab. The target is a loudspeaker placed inside one of the offices. Even while the robot moves along the corridor, its target representation already engages an approximate representation of the sound source. Based on that representation and helped by obstacle avoidance, the robot moves through the office door. It circumnavigates a number of additional obstacles and eventually finds the sound source, which is "hidden" inside a box with only a single entrance. It stops in front of the sound source (controlled by the velocity dynamics). Thus, although the architecture does not have global plans and finding a path is not theoretically guaranteed, the robot finds a remote target by moving along surfaces with the help of obstacle avoidance, until an "entry" is found. In our practical experience, we have found it difficult to create scenarios in which the robot does not find its way even to quite intricately hidden sound sources.

8. Discussion

We have demonstrated how dynamic fields can provide robotic systems with subsymbolic representations that rely on low-level sensory information. These representations enable the robot to show the simplest forms of cognitive capabilities, such as detecting targets, estimating direction to a target through interpolation, stabilizing a decision as to which of multiple targets to track, maintaining targets in short-term memory during momentary removal of pertinent sensory information, and deleting memory items after a characteristic delay to clear the memory of obsolete information. In the implementation, the dynamic field enabled a small autonomous vehicle to find sound sources while avoiding obstacles. Memory helped with intermittent sound, decision making enabled tracking of a sound source even if obstacle avoidance increased momentarily the distance from the sound source. Detection led to stable behavior near the sensor threshold.

The demonstrated robotic system has a number of obvious applications. We played, for instance, with the human voice as a sound source and demonstrated that the robot can follow or

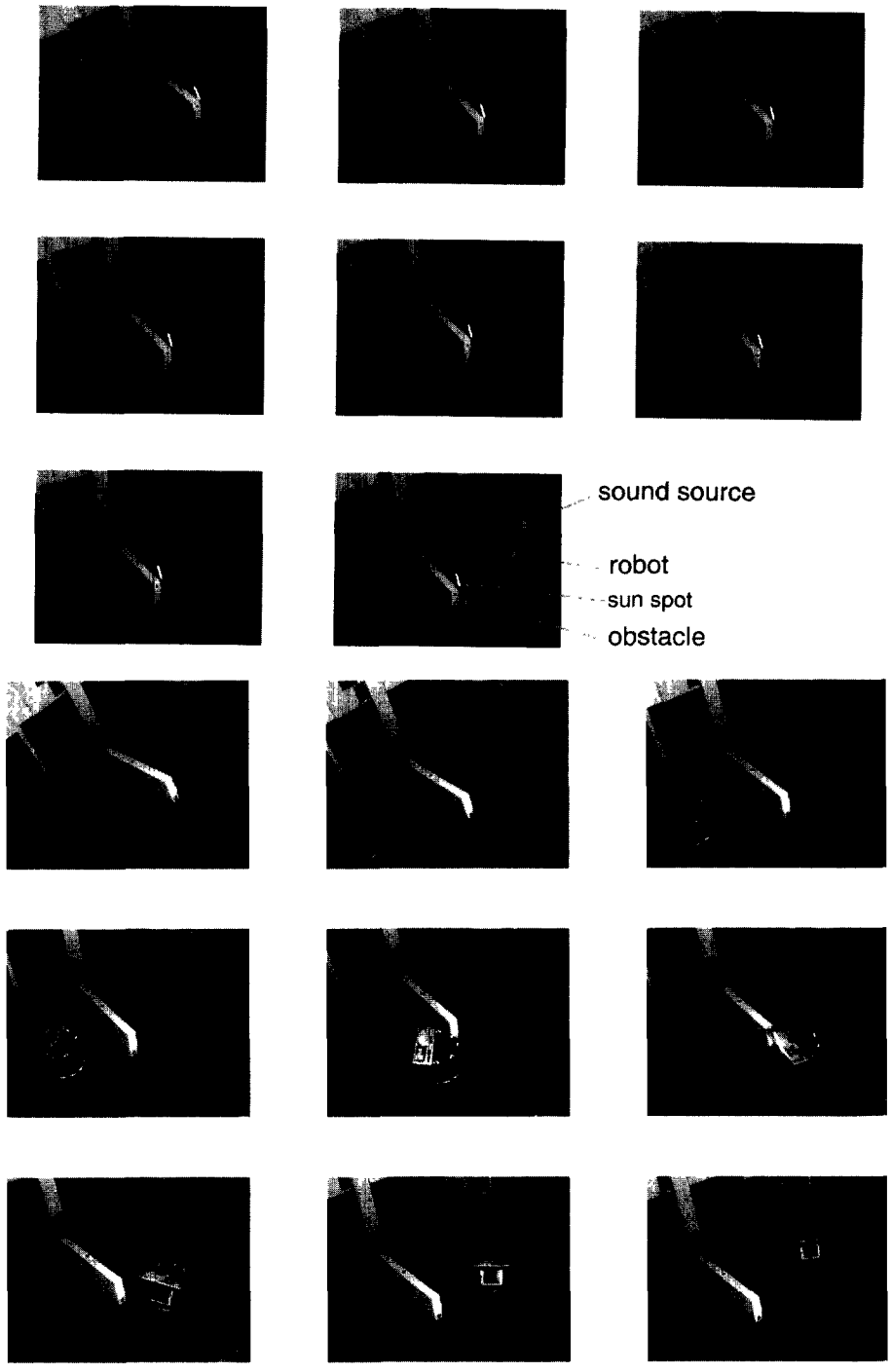

Fig. 18. A sequence of video images illustrates the motion of the robot. Time increases from top to bottom, first along the first raw, then along the second raw, and so on. The robot is the cylindrical object, located in the first frame in the lower left corner. A loudspeaker is visible in the top right corner. A long obstacle makes a barrier in between the robot initial position and the loud speaker. The sound source is on all the time but exhibits some moments of silence. The top shows that the robot moves smoothly around the obstacle, to the left, toward the sound source, coming to rest in the final frame in front of the loud speaker. The bottom shows a new run. This time the robot turns around the obstacle to the right, steering toward the sound source, and it comes to rest near the loudspeaker.

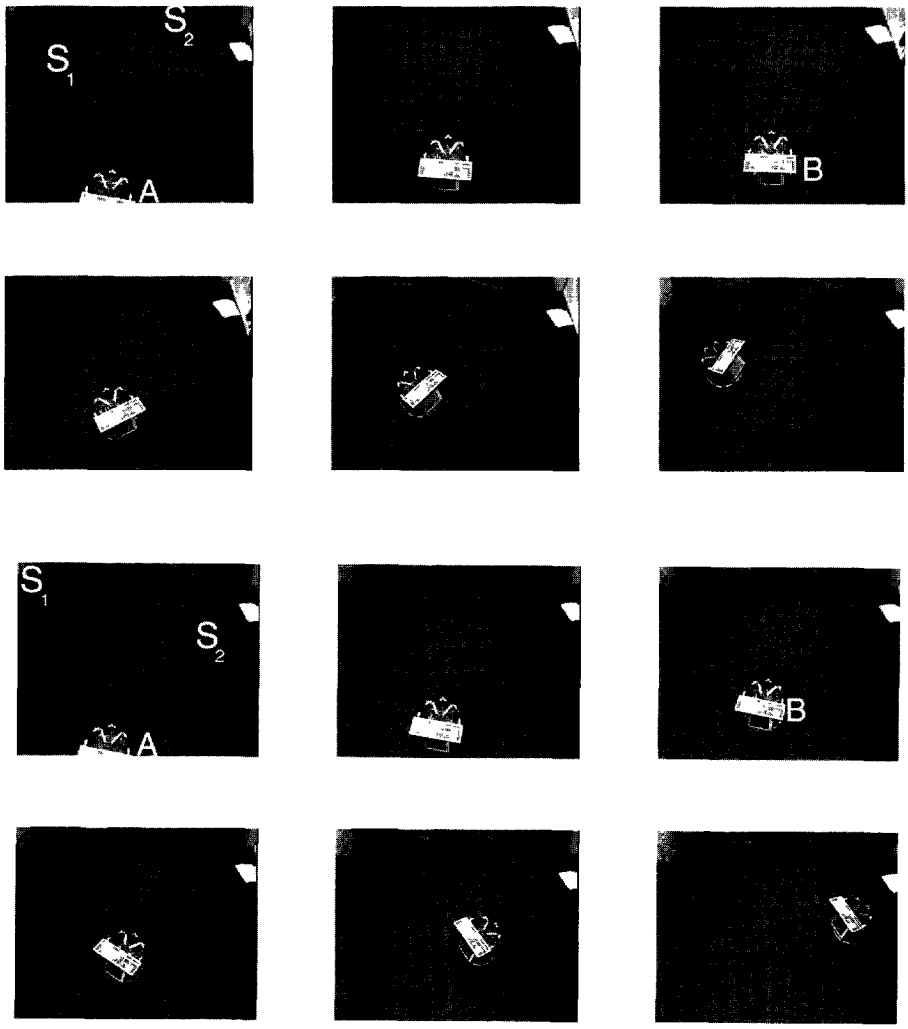

Fig. 19. Two sequences of video images show the robot behavior in the presence of two loud speakers emitting the same sound and in an asymmetric configuration. Time increases as announced in Figure 18. The robot is first located as depicted on the first frame. Two loud speakers, S_1 and S_2, are located near the left and right top corners, respectively. Initially, the sound sources are turned off, thus the robot moves straightforward. When it has traveled a distance of 1 meter, both sound sources are switched on. In part(a), the loud speaker on the left, S_1, is closer to the robot. This sound source is thus selected (it is visible in the fourth frame), and the robot moves smoothly toward it, coming almost to a stop near the loud speaker S_1. In part (b), another run is shown. Here the loud speaker on the right, S_2, is closer to the robot. Analogously, the robot selects the closest sound (the decision can be seen in frame 4) and moves toward it.

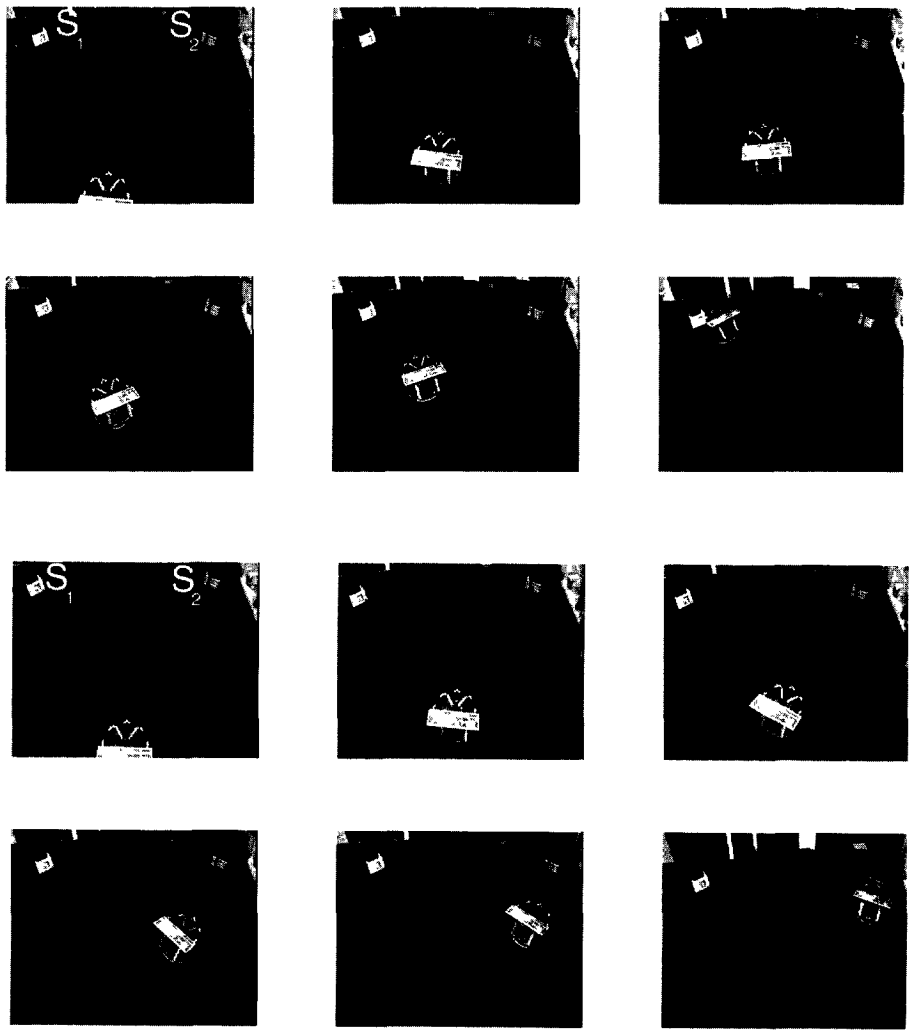

Fig. 20. The two loudspeakers are now placed at exactly the same distance to the robot. In the run illustrated in part (a), the random fluctuations favor the selection of the leftmost target, S_1. The decision starts being visible on the third frame. The robot moves toward S_1 and finally stops in front of the loud speaker (final frame). Part (b) shows a new run. This time the random fluctuations favor the selection of the right target, S_2. This decision becomes visible on the third frame. Again the robot moves toward the selected sound source and comes to rest in front of it.

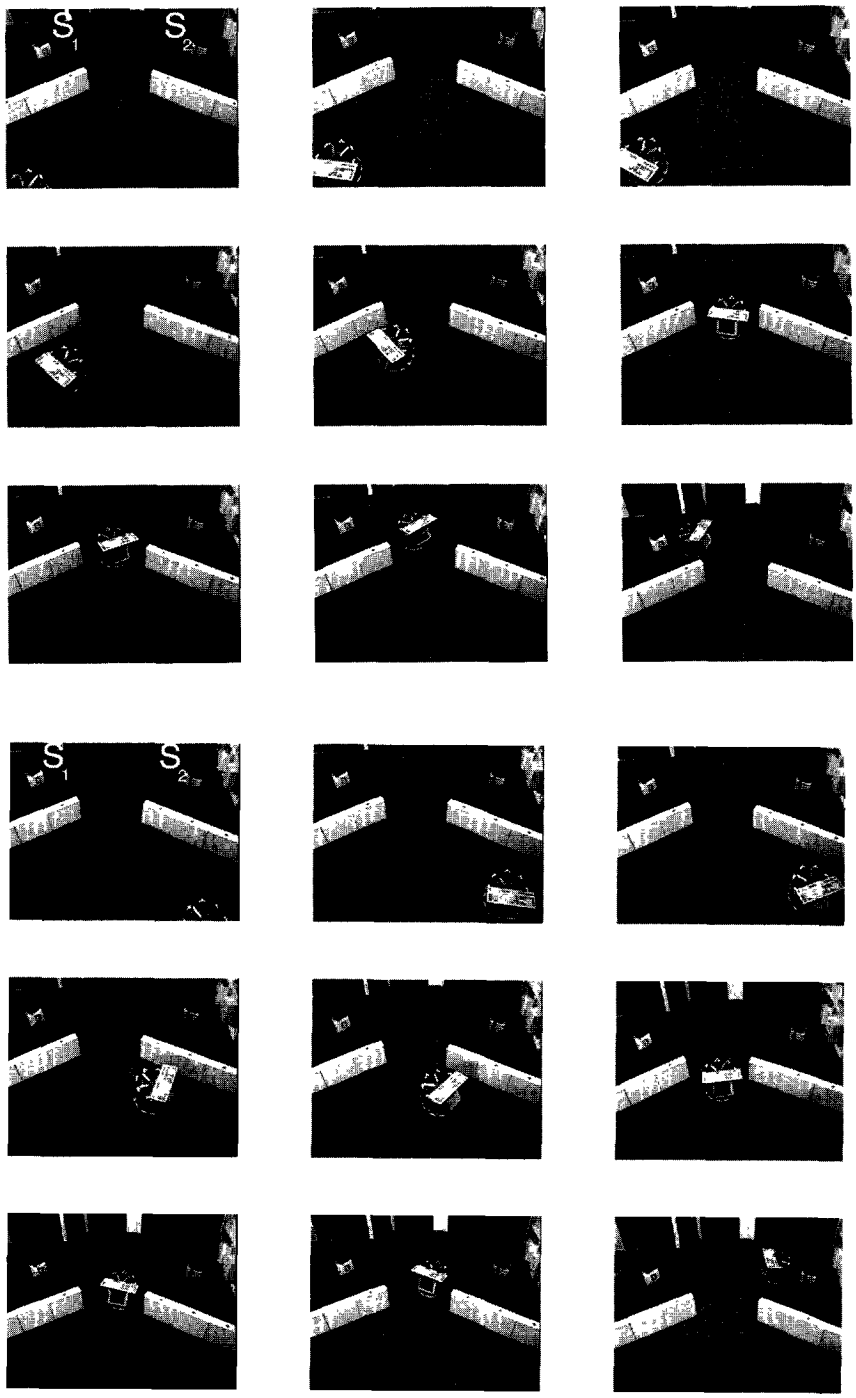

Fig. 21. This figure shows that hysteresis enables to maintain a decision stable. Two sequences of video images are presented. The two equal sound sources, S_1 and S_2, are now placed behind obstacles as can be seen on the first frame. In part (a), the robot initial position is the left bottom corner in the first frame, i.e., in this run the robot is initially closer to the sound source on the left, S_1. Thus, the field evolves a peak of activation at the leftmost target direction. While moving toward S_1, due to the obstacle configuration, the robot is forced to pass through the opening in between the two barriers. At this time (frame 6), the sensory information received from the two sound sources is symmetric and the input to the field is bimodal with two input peaks of equal amplitude. The preexisting peak on the field corresponding to the selection of the left target bias the competition toward retaining the leftmost target. Thus, the decision of moving toward S_1 is maintained stable. Part (b) shows a similar run. The robot is now closer to the rightmost target (see first frame). The robot starts moving toward the location of this sound source (but constrained of course by the obstacles). This decision is maintained stable when the robot is confronted with symmetric bimodal sensory input (frame 6). The robot comes to rest in front of the loud speaker S_2 (frame 9).

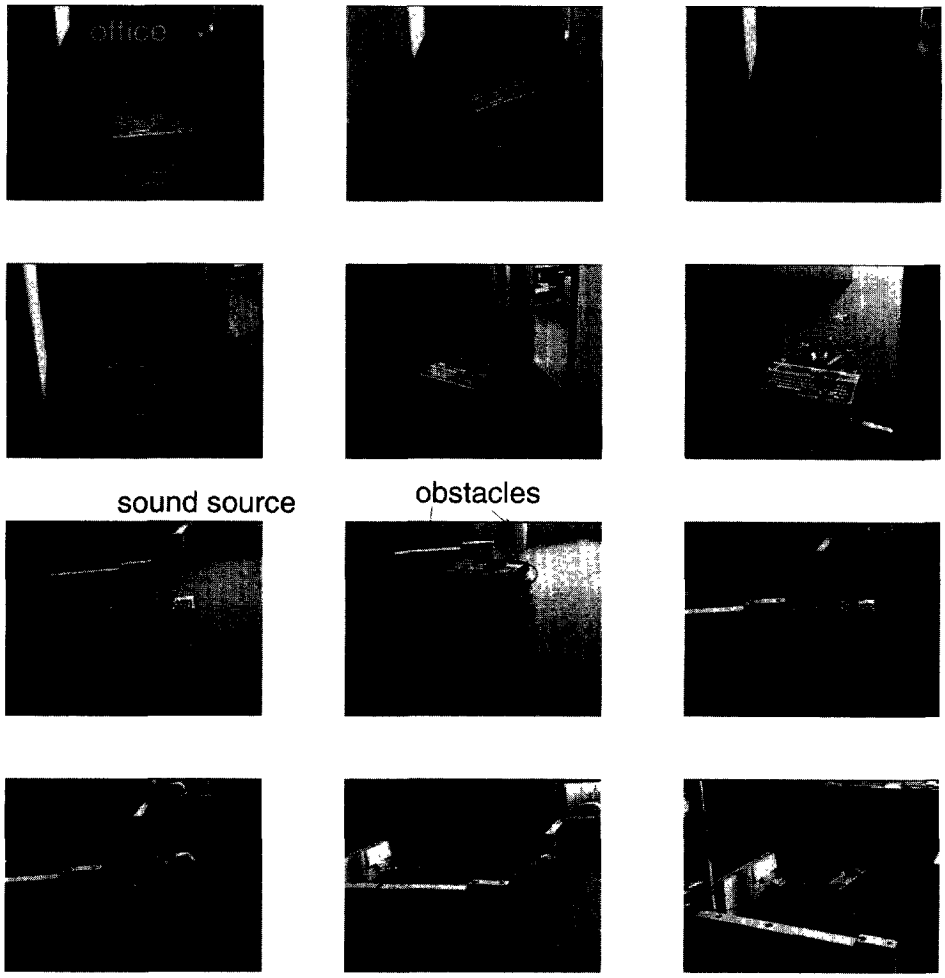

Fig. 22. This figure shows a video sequence of the robot behavior in a more complex environment. The robot is initially positioned in the corridor. A sound source is inside one of the offices as indicated in the first frame. The robot moves along the corridor (frame 1 to frame 4). When the robot approaches the office door, the phonotaxis behavior makes it enter into the room (frame 6). In frame 7, the robot is faced with a barrier of obstacles between it and the sound source. The sound source is visible on the left top corner of this frame. The robot moves around the obstacles toward the target and finally comes to near rest in front of the loud speaker (last frame).

move toward a human operator who every now and then voices an utterance. The memory capacity of the dynamic field keeps the direction toward the human operator active during the intervals of silence. This robot system thus demonstrates an interesting interface, which could have multiple uses. Toys are an obvious example. An autonomous platform carrying tools and being operated by calling out is another example. Household devices to support handicapped people could be another domain in which such a simple interface could be of use. By installing particular filters at the auditory level, this system could be made sensitive to only particular types of sound (e.g., human voices rather than ambient sound).

The principle of representing direction information obtained from low-level sensors could also be used to generate more complex movement behaviors of robotic platforms. For instance, the vehicle can be made to steer at a particular angle with respect to a sound source. In this way, a group of robots could drive in formation, if each robot emits a sound. Maneuvers in front of a docking station could be based on this mechanism. The representation of direction could also be used as a means of recalibrating robot orientation without the need for actual movement of the robot into a particular position or orientation. Finally, the fact that the sensed angle is explicitly represented could be used to communicate that information among robots or to an operator, which makes it possible to integrate such information into more complex strategies, for instance, for multirobot environments.

Sound is only one sensory channel on which this approach can be based. We have tested a similar architecture that was based on light sensors (three light-dependent resistors). That system was able to orient toward light sources (Bicho and Schöner 1997b). The fact that there is typically much more ambient light than ambient sound in work environments makes this a useful architecture only for work in near darkness, however. Chemodetection is another potential sensor system that could be enhanced through a dynamic field (Kuwana and Shimoyama 1998).

One limitation of the system as it stands comes from the computational demands of the dynamic fields. The cycle time obtained for a computational step on the order of 100 ms leads to reasonably fast behavior, but one could be much faster. If more complex architectures were tried with multiple dynamic fields for different representations, then this could become a serious limitation. One solution might be to implement the computationally critical parts in assembler code. Another approach might be to use more optimal numerical procedures.

There are, of course, limitations that come from the low-level sensor system. The robot may select, for instance, sometimes an echo rather than the real sound source. This is not severe, however, as echoes do not persist as the robot changes position. Once the robot has latched onto the real target, the stabilization of decision making provided by the dynamic field makes sure that the robot does not get sidetracked by new echoes it encounters on the way to the target.

Appendix

Field Parameters

$d\psi = 8.0$ deg
$k_p = 2.0$
$k_n = 3.5$
$l_{coop} = 40$ deg
$\tau = 5dt$ (where dt is the cycle time in seconds)
$W_m = 0.7$
$h_{\min} = -0.77$
$h_{\max} = -0.0875$
$r_{h,\min} = 1/(5\tau)$
$r_{h,\max} = 1/(50\tau)$
$M_o = 0.25$
$\sigma = 0.4$

Target Acquisition

$\lambda'_{tar} = 1/(5\tau)$

Obstacle Avoidance

$\beta_1 = 5\lambda'_{tar}$
$\beta_2 = 20$
$R_{robot} = 25$ cm
$\Delta\theta = 30$ deg

Velocity Control

$c = 100$
$c_{v,tar} = 15\lambda'_{tar}$
$c_{v,obs} = 10\lambda'_{obs}$

Acknowledgments

This project was supported, in part, through grant PRAXIS XXI/BD/2949/94 from the FNICT (Portugal) and the GIS "Sciences cognitives" (France). Discussions with Wolfram Erlhagen, Axel Steinhage, and Martin Giese are gratefully acknowledged. We thank Geza Lorenz for her help with the digitalization of the video images and Nicolas Mathian for help during the experiments. We thank Professor von Seelen for making the facilities of the Institut für Neuroinformatik in Bochum available during temporary visits of E. B. Professors Carlos Couto and Francisco Vaz are thanked for their continuing institutional support.

References

Amari, S. 1977. Dynamics of pattern formation in lateral-inhibition type neural fields. *Biological Cybernetics* 27:77–87.

Arkin, A. R. 1998. *Behavior-Based Robotics*. Cambridge, MA: MIT Press.

Bicho, E. 1999. *Dynamic Approach to Behavior-Based Robotics*. Ph.D. thesis, University of Minho, Portugal.

Bicho, E., Mallet, P., and Schöner, G. 1998. Using attractor dynamics to control autonomous vehicle motion. *IECON'98,24th Annual Conference of the IEEE Industrial Electronics Society*, Aachen, Germany, August 31-September 4, vol. 2, pp. 1176–1181.

Bicho, E., and Schöner, G. 1997a. The dynamic approach to autonomous robotics demonstrated on a low-level vehicle platform. *Robotics and Autonomous Systems* 21:23–35.

Bicho, E., and Schöner, G. 1997b. Target position estimation, target acquisition, and obstacle avoidance. *Proceedings of the IEEE International Symposium on Industrial Electronics (ISIE'97)*, Piscataway, NJ, pp. SS13–SS20.

Blauert, J. 1996. *Spatial Hearing - The Psychophysics of Human Sound Localization*. Cambridge MA: MIT Press.

Braitenberg, V. 1984. *Vehicles. Experiments in Synthetic Psychology*. Cambridge, MA: MIT Press.

Brooks, R. A. 1991. Intelligence without representation. *Artificial Intelligence* 47:139–160.

Cade, W. H., and Cade, E. S. 1992. Male mating success, calling and searching behavior at high and low densities in the field cricket, gryllus integer. *Animal Behavior* 43:49–56.

Chatila, R. 1994. Representations + reason + reaction → robot intelligence. In *Robotics Research — Tthe Sixth International Symposium*, ed. T Kanade and R Paul, 387–397. Cambridge, MA: The International Foundation for Robotics Research.

Chipalkatti, R., and Arbib, M. A. 1987. The prey localisation model: A stability analysis. *Biological Cybernetics* 57:287–299.

Connell, J. H. 1990. *Minimalist Mobile Robotics*. New York: Academic Press.

Duda, O. 1996. Auditory localization demonstrations. *Acustica - Acta Acusticca* 82:346–355.

Engels, C., and Schöner, G. 1995. Dynamic fields endow behavior-based robots with representations. *Robotics and Autonomous Systems* 14:55–77.

Ewert, J.-P. 1974. The neural basis of visually guided behavior. *Sci. Am.* 230:34–42.

Guentchev, K. Y., and Weng, J. 1998. Learning-based three dimensional sound localization using a coplanar array of microphones. *Intelligent Environments Symposium, Proc. 1998 AAAI Spring Symposium Series*, Stanford University, March 23-25.

House, D. H. 1988. A model of the visual localization of prey by frog and toad. *Biological Cybernetics* 58:173–192.

Kishimoto, K., and Amari, S. 1979. Existence and stability of local excitations in homogeneous neural fields. *Journal of Mathematical Biology* 7:303–318.

Kopecz, K., and Schöner, G. 1995. Saccadic motor planning by integrating visual information and pre-information on neural, dynamic fields. *Biological Cybernetics* 73:49–60.

Kuwana, Y., and Shimoyama, I. 1998. A pheromone-guided mobile robot that behaves like a silkworm moth with living antennae as pheromone sensors. *International Journal of Robotics Research* 17(9):924–933.

Large, E., Christensen, H. I., and Bajcsy, R. 1999. Scaling the dynamic approach to path planning and control: Competition. *International Journal of Robotics Research* 18:37–58.

Liggins, M., Kadar, I., and Vannicola, V. 1997. Distributed fusion architectures and algorithms for target tracking. *Proc. of the IEEE*, vol. 85, January.

Lund, H. H., Webb, B., and Hallam, J. 1997. A robot attracted to the cricket species *Gryllus bimaculatus*. In *Fourth European Conference on Artificial Life*, ed. P Husbands and I Harvey, pp. 246–255. Cambridge, MA: MIT Press.

Mills, A. 1972. Auditory localization. *Foundations of Modern Auditory Theory* 2:301–348.

Perko, L. 1991. *Differential Equations and Dynamical Systems*. Berlin: Springer-Verlag.

Schöner, G., and Dose, M. 1992. A dynamical systems approach to task-level system integration used to plan and control autonomous vehicle motion. *Robotics and Autonomous Systems* 10:253–267.

Schöner, G., Dose, M., and Engels, C. 1995. Dynamics of behavior: Theory and applications for autonomous robot architectures. *Robotics and Autonomous Systems* 16:213–245.

Shama, S., Shen, N., and Gopalawamy, P. 1989. Stereausis: Binaural processing without neural delays. *Journal of the Acoustical Society of America* 86(March):989–1006.

Steinhage, A. 1998. *Dynamical Systems Generate Navigation Behavior*. Ph.D. thesis. In Berichte aus der Physic. Aachen, Germany: SHAKER-Verlag.

Steinhage, A., and Schöner, G. 1997. Self-calibration based on invariant view recognition: Dynamic approach to navigation. *Robotics and Autonomous Systems* 20:133–156.

Webb, B. 1995. Using robots to model animals: A cricket test. *Robotics and Autonomous Systems* 16:117–134.

Wilson, H. R., and Cowan, J. D. 1973. A mathematical theory of the functional dynamics of cortical and thalamic nervous tissue. *Kybernetik* 13:55–80.